Scaling head-neck response data for biofidelity assessment of the small female WorldSID

Wisgerhof, R.P.

Award date:
2007

Scaling head-neck response data for biofidelity assessment of the small female WorldSID

R.P. Wisgerhof
Master Thesis Mechanical Engineering
MT 07.38
October 2007

Committee:

prof. dr. ir. J.S.H.M. Wismans (TU/e, TNO)
prof. dr. ir. M.G.D. Geers (TU/e)
dr. ir. J.A.W. van Dommelen (TU/e)
dr. ir. I.J.M. Besselink (TU/e, TNO)
ir. R. Meijer (TNO)

Eindhoven University of Technology
Department of Mechanical Engineering
Division of Automotive Engineering Science

TNO Science and Industry
Business Unit Automotive
Department of Integrated Safety

Abstract

In the European project APROSYS subproject 5 'Biomechanics', a small female Worldwide Side Impact Dummy (WorldSID), further referred to as 5th WS, is being developed. The peak head responses of the 5th WS prototype did not all meet the scaled head-neck response requirements during full-scale sled tests in the lateral NBDL setup. These head-neck response requirements are scaled from responses measured on male volunteers according to the head-neck response scaling method proposed by Irwin et al. (2002). It was found that the most possible reason for the discrepancy is that the scaling rules are not valid. To investigate this, two objectives were formulated for the present study. The first objective is to analyse the head-neck scaling method of Irwin et al. (2002) for both geometry as well as response, and if necessary, develop new response requirements. The second objective is to evaluate of the head-neck design and responses of the 5th WS according to the valid requirements.

To investigate the validity of the head-neck scaling method of Irwin et al., (2002) an extensive literature study on the differences in both head-neck anthropometry as well as head-neck responses between males and females was carried out. It was found that males can exert higher forces with their neck muscles than females can. However, if no pretension of the neck muscles is present, the time it takes to reach this maximum force is greater than the time to maximum head excursion. Therefore, the difference in possible neck stiffness does not have to be accounted for in scaling the head-neck responses in an unexpected, lateral impact like for instance, the lateral NBDL tests.

New scaling rules were derived to formulate new head-neck response requirements for biofidelity assessment of the 5th WS. This is, since the current requirements of Irwin et al. (2002) are based on the faulty found assumption that the neck stiffness of midsize males is larger than that of small females in the lateral NBDL setup. To eliminate the influence of the shoulder design of the dummy, the head-neck system should be tested separately, using an acceleration signal of the first thoracic vertebra, T1, as input.

To evaluate the head-neck design, simulations with a newly developed numerical head-neck model of the 5th WS have been carried out in MADYMO. The numerical head-neck model of the 5th WS was scaled down from a well-validated numerical model of the midsize male WorldSID, further referred to as 50th WS. It was found that the head responses of the numerical model of the 5th WS meet the newly developed requirements well, indicating that the neck has 'good' biofidelity. The head responses of this model were also compared to the corresponding head responses of a numerical model of the 50th WS. The found differences in head responses between both numerical models were comparable to the difference between the response requirements for the midsize male and those for the small female, developed during this study. This confirms the consistency of the newly developed response requirements.

Samenvatting

In het Europese project APROSYS wordt een kleine vrouwelijke dummy ontwikkeld voor laterale impact (WorldSID), deze wordt hier 5th WS genoemd. De piek responsies van het 5th WS prototype in laterale NBDL configuratie voldeden niet allemaal aan geschaalde hoofd-nek responsie-eisen. Deze responsie-eisen zijn geschaald naar de gemeten responsies van mannelijke vrijwilligers volgens de schalingsmethode voor hoofd- en nek responsies opgesteld door Irwin et al. (2002). Uit een eerste evaluatie bleek dat de geschaalde eisen waarschijnlijk niet correct zijn voor deze test configuratie. In deze studie is dit onderzocht aan de hand van twee onderzoeksdoelen. Ten eerste wordt de hoofd-nek schalingsmethode van Irwin et al. (2002) geanalyseerd om te bepalen of deze methode toe te passen is op de NBDL test set-up. Indien dit niet het geval is, worden nieuwe schalingsregels en nieuwe responsie-eisen opgesteld. Ten tweede wordt het hoofd-nek systeem van de 5th WS geëvalueerd met behulp van de correcte response eisen.

Om te onderzoeken of de schalingsmethode voor hoofd- en nek responsies van Irwin et al. (2002) toegepast kan worden, is er een uitgebreide literatuurstudie gedaan naar zowel verschillen in hoofd- en nek anthropometrie als verschillen in hoofd- en nekresponsies tussen mannen en vrouwen. Mannen kunnen meer kracht uitoefenen met hun nekspieren dan vrouwen. Echter, wanneer de nekspieren voor de test niet aangespannen zijn, is de tijdsduur om tot maximale nekkracht te komen langer dan de tijdsduur tot maximale verplaatsing van het hoofd. Daarom hoeft dit verschil in maximale nekstijfheid niet meegenomen te worden bij het schalen van de hoofd- en nekresponsies in een onverwachte, laterale impact zoals de laterale NBDL test.

Nieuwe schalingsregels zijn afgeleid om nieuwe responsie-eisen voor het hoofd en de nek op te stellen, omdat de huidige responsie-eisen van Irwin et al. (2002) zijn gebaseerd op de onjuiste aanname dat de stijfheid van een mannennek groter is dan die van een vrouwennek in de NBDL test configuratie. Om de invloed van het schouderontwerp van de dummy te elimineren, wordt het hoofd-nek systeem apart getest door een acceleratie van de bovenste borstwervel, T1, voor te schrijven.

Om het ontwerp van het hoofd en de nek te onderzoeken zijn er simulaties met een numeriek hoofd-nek model van de 5th WS uitgevoerd in MADYMO. De responsies van het hoofd van dit model voldoen aan de eisen die in dit onderzoek zijn opgesteld. Het numerieke model van het hoofd-nek systeem van de 5th WS is geschaald van het numerieke model van de gemiddelde mannelijke WorldSID, de 50th WS, dat uitgebreid gevalideerd is voor laterale belasting. De responsies van het numerieke hoofd-nek model van de 5th WS zijn vergeleken met die van het numerieke model van de 50th WS. De gevonden verschillen in hoofd responsie tussen beide numerieke modellen waren vergelijkbaar met de verschillen tussen de responsie-eisen voor de gemiddelde man en de kleine vrouw, die in dit onderzoek zijn opgesteld. Dit bevestigt de consistentie van de nieuwe responsie-eisen.

Contents

1. Introduction

1.1 Problem definition

In car-to-car crashes, side impact is the most severe and second frequent traffic accident configuration (Samaha and Elliot, 2003). The head is often seriously injured in this crash scenario, due to interaction with the vehicle structure. Although neck injuries are generally not the most frequent injuries occurring in side impact, the behavior of the neck is very important since it determines the trajectory of the head (Been et al., 2004). To accurately investigate the behavior of occupants during a crash, the development of biofidelic side impact test devices, also called dummies, is important.

A midsize male Worldwide Side Impact Dummy (WorldSID), further referred to as 50th WS, which has good head-neck biofidelity has been developed. In the European project APROSYS subproject 5 'Biomechanics', the development of a small female WorldSID is in progress. It represents a part of the population that is often at highest risk but yet not well accounted for in regulatory crash testing (Barnes et al., 2005). Within this project the objective of TNO is to evaluate the behavior of the head-neck system of the small female WorldSID, further referred to as 5th WS.

The head-neck biofidelity of side impact dummies is assessed according to the response requirements for the head-neck system measured on midsize male human subjects published in ISO TR 9790.

Since there are no side impact tests available of small female human subjects, the head-neck response requirements for the 5th WS were scaled from those of the 50th WS. The scaling was performed using the scaling rules of Irwin et al. (2002), further referred to as Irwin. The scaled head-neck requirements are used to assess the biofidelity of the head-neck response of the 5th WS prototype. However, the results of the tests with this prototype showed that the measured peak values of these responses do not all correspond with the scaled requirements (Meijer et al., 2007). It was found that the most possible reason for this discrepancy is that the scaling rules that were used to scale the response requirements for the head-neck system are not valid.

1.2 Objectives

The first and most important objective of this study is to perform a thorough analysis of the scaling method for the head-neck system as proposed by Irwin et al. (2002), to provide a judgement on its validity. From this analysis it will be clear if it is necessary to derive new scaling rules and new response requirements for the 5th WS.

The second objective is to evaluate the design and response of the head-neck system of the 5th WS according to the valid response requirements. This part will be done by means of simulations with the multi-body software MADYMO.

1.3 Outline of the report

A literature review which presents background information about the anatomy of head and neck, as well as the development and biofidelity assessment of both the midsize male WorldSID and the small female WorldSID is presented in chapter 2. The head-neck scaling method of Irwin is also presented in this chapter.

The analysis of the scaling method for the head-neck system as proposed by Irwin, is described in chapter 3. Among others, this chapter contains a review on the anthropometric differences between males and females with respect to their head and neck, as well as differences in their head-neck response in lateral direction. Conclusions on the validity of the head-neck scaling rules according to Irwin, are presented in its last sections.

The evaluation of the design of the head-neck system of the 5th WS will be discussed in chapter 4 of this report. Results of simulations with an available, validated numerical model of the 50th WS and those of simulations with a newly developed numerical model of the 5th WS in MADYMO will be presented. A schematic overview of chapter 3 and 4 is shown in Figure 1.1.

Conclusions and recommendations of this study are presented in section 5 of this report.

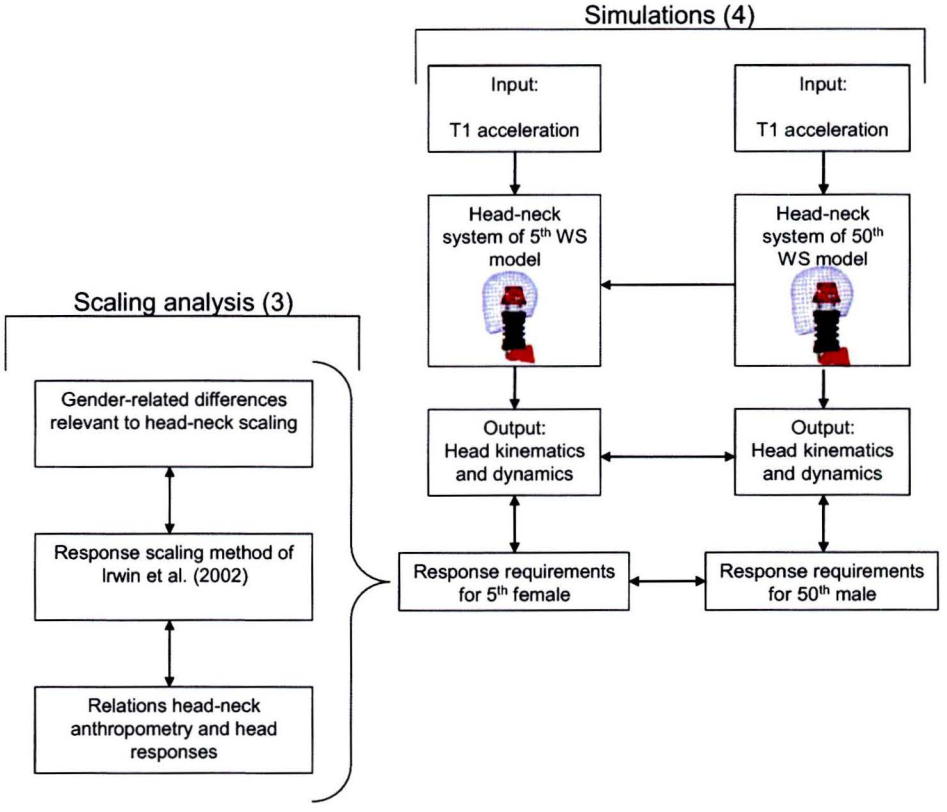

Figure 1.1 Schematic overview of chapter 3 and 4

2. Literature review

2.1 Anatomy

The human spine consists of three parts: the lumbar, the thoracic and the cervical spine, as given in Figure 2.1. The spinal column provides protection to the spinal chord and is the load bearing structure of the head and torso. The whole spine consists of 5 lumbar, 12 thoracic and 7 cervical vertebrae. The cervical spine, representing the neck, is responsible for the movement of the head. The 7 cervical vertebrae can anatomically and functionally be divided in two parts, C1-C2 and C3-C7. C1, also named Atlas, is a ring of bone and has a pair of facets on the superior side. These articulate with the base of the skull, the occipital condyles, OC, shown in Figure 2.2. This joint is responsible for the frontal and lateral rotation of the head relative to the neck. C2, also called Axis, has a small process of bone, the dens, at the superior side. This dens fits in the anterior side of the vertebral foramen of the atlas. This joint allows rotational movement around the vertical axis of the head. Atlas and axis are displayed in Figure 2.3. The other cervical vertebrae, C3 to C7, are very much alike as can be seen in Figure 2.4.

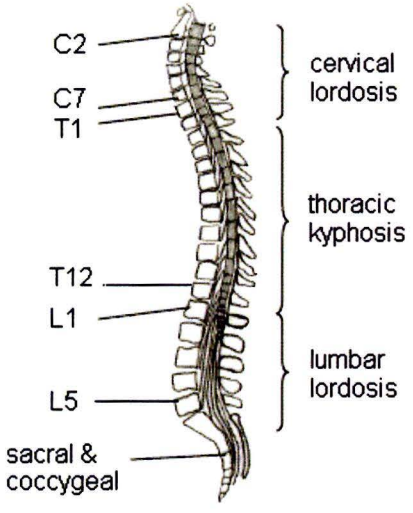

Figure 2.1 Schematic representation of the spine (side view) (www.neurosurgeon.org)

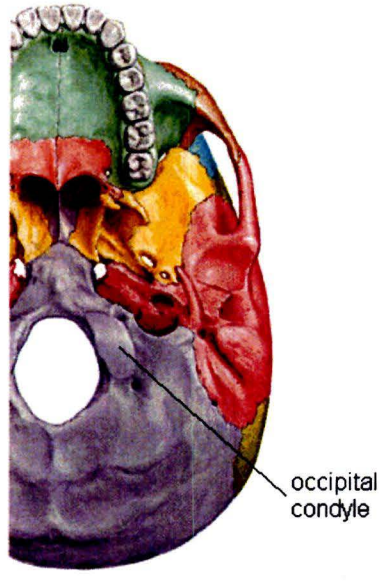

Figure 2.2 Cranial base of the skull (inferior view) (Dally, 1998)

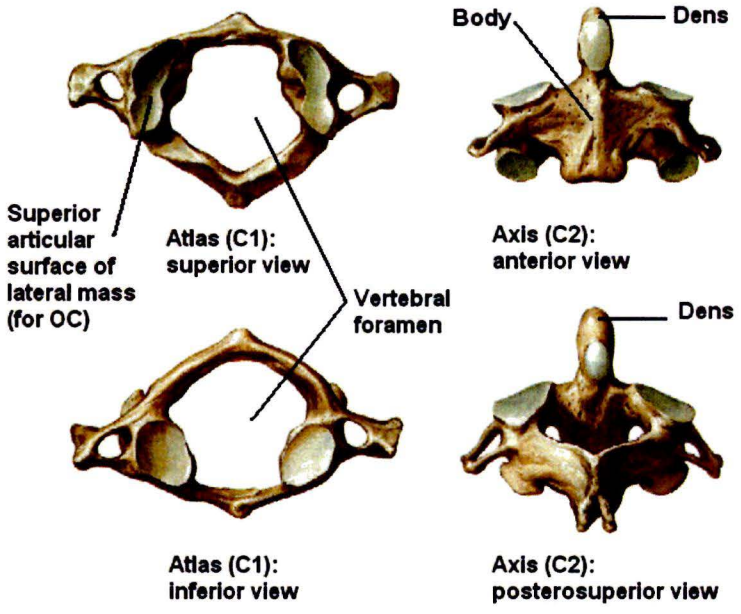

Figure 2.3 Anatomy of C1 (Atlas) and C2 (Axis) (Dally, 1998)

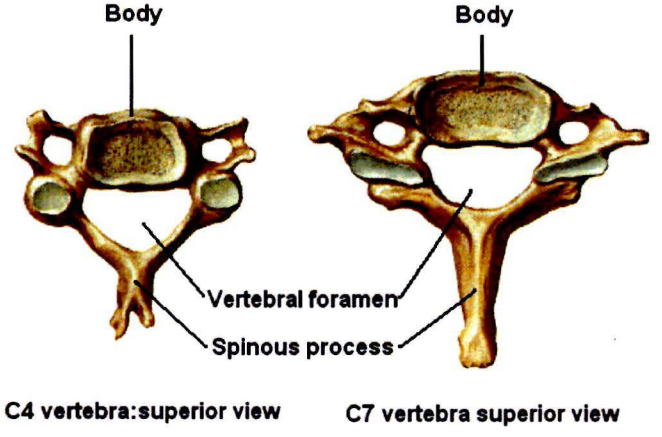

Figure 2.4 Anatomy of C4 to C7 (Dally, 1998)

The vertebrae are separated by intervertebral discs and connected with soft tissue like ligaments and muscles. These mainly provide the tensile properties of the neck. The interaction between all cervical vertebrae and between the vertebrae and the head determine the motion of the head.

2.2 50th male WorldSID

2.2.1 History

When the first WorldSID prototype was assembled in September 2000, a first step was taken towards a new, highly biofidelic, advanced side impact crash test dummy that could be used for worldwide side impact regulation. This WorldSID, shown in Figure 2.5, has the anthropometry of a midsize male, also called a 50th percentile dummy. Here, with 50th percentile dummy is meant that 50 percent of the population has a smaller length and 50 percent is taller, and 50 percent of the population has a smaller weight and 50 percent has a larger weight than this dummy. The biofidelity of the 50th percentile male WorldSID (50th WS) has been evaluated against established response requirements for the critical body regions in side impact. These response requirements are defined in the International Organization of Standardization Technical Report 9790 (ISO TR 9790).

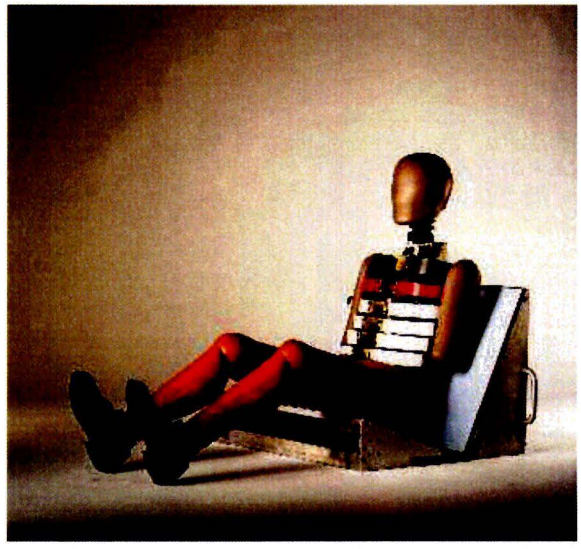

Figure 2.5 50th percentile male WorldSID (www.worldsid.org)

2.2.2 Head-neck design

Mass, dimensions, inertia and center of gravity of each body segment of the dummy were designed using the database of Schneider et al. (1983). This database consists of measurements on 13645 US citizens of different age and proportion. Based on this database the hardware head-neck is designed as shown in Figure 2.6.

Figure 2.6 Head-neck system of the 50th male WorldSID (ISO TGN393)

The WS head is a featureless, seamless, combined skull/skin assembly. Herein it differs from other crash test dummies. The head is made seamless to prevent any unrealistic interaction with the vehicle interior. The aluminum instrumentation core, which is equipped with acceleration instrumentation for every direction, is inserted into the head cavity through the base of the head. Figure 2.7 shows the location of the instrumentation core as well as the locations of the center of gravity (CG) of the head and the OC. The neck is attached to the head at the OC joint and to the torso at the C7-T1 location. The complete neck assembly is shown in Figure 2.8. The neck is based on the ES-2 dummy neck, but some modifications are made. Special buffers are introduced to optimize the neck for frontal flexion and extension and to provide torsional stiffness. Together with half-spherical screws, the upper and lower neck interface plates form two spherical joints, located at the anthropometric position of respectively the OC and of first thoracic vertebra, T1. Load cells are located at the OC and T1.

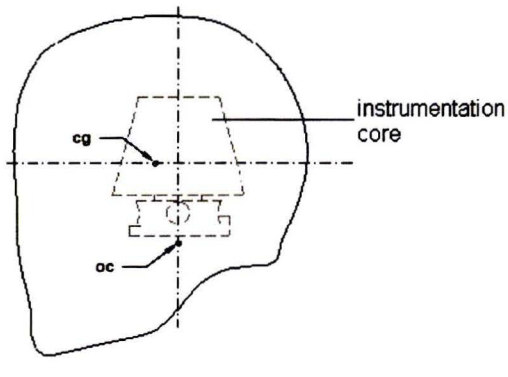

Figure 2.7 WorldSID head assembly (ISO TGN399)

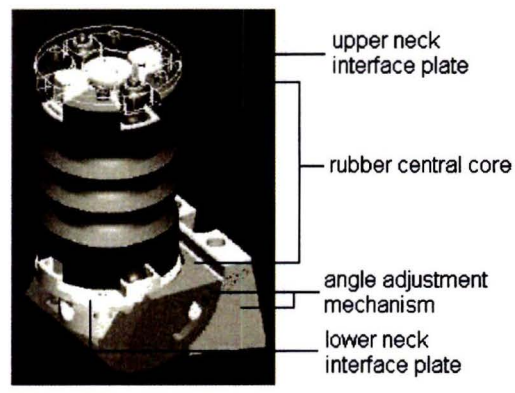

Figure 2.8 WorldSID neck assembly (Been et al., 2004)

2.2.3 Assessing lateral head-neck biofidelity

Several sled tests have been performed by various institutes to measure and analyse the motion of the head-neck system. From these studies, response requirements are obtained which are used to assess the biofidelity of crash test dummies. This has already been done for frontal dummies, for example the Hybrid III. Nowadays, also side impact dummies are validated using requirements from similar studies.

ISO TR 9790 contains test methods to assess the biofidelity of all critical parts of a side impact dummy as well as the biofidelity of the whole dummy. Three different tests for assessing the biofidelity of the neck are integrated into ISO TR 9790: the Patrick and Chou test (Patrick and Chou, 1976), the Tarriere test (Tarriere, 1986) and the NBDL test (Ewing et al., 1977).

Patrick and Chou (1976) measured the head-neck response of midsize male volunteers using a decelerator sled. The volunteers were seated on a rigid chair, of which the back was rotated 15 degrees rearward. The seat was mounted sideways on a sled that was accelerated slowly up to a velocity of 5.8 m/s and abruptly decelerated with a constant deceleration level of 6.7*g*, with *g* being the standard gravity. The response data from the most severe test were used to specify the dummy response requirements presented in Table 2.1.

Table 2.1 Response requirements of Patrick and Chou (1976)

Requirements 50th Male	Unit	Test SAE 156	Lower Bound	Upper Bound
Peak flexion angle	deg	43.2	40	50
Peak bending moment about A-P Axis at OC	Nm	45.2	40	50
Peak bending moment about R-L Axis at OC	Nm	26.2	20	30
Peak twist moment	Nm	17.4	15	20
Peak shear force at OC	N	794	750	850
Peak tension force at OC	N	387	350	400
Peak P-A shear force	N	351	325	375
Peak resultant head acc	*g*	21.0	18	24

Tarriere (1986) conducted four high *g*-level tests using midsize male Post Mortem Human Subjects (PMHS) to obtain data to define the lateral neck bending response in a more severe test environment than possible for volunteer testing. However, every test had an abnormality. Despite the fact that the PMHS's neck was fractured in test MS 249, Tarriere selected this test as the most appropriate one for defining a set of response requirements, given in Table 2.2. The results of this test were modified to reflect the human response. This was done by comparing the responses of the PMHS to volunteer responses in low-*g* tests.

Table 2.2 Response requirements of Tarriere (1986)

Requirements 50th Male	Unit	MS 249	Lower Bound	Upper Bound
Peak lateral acc T1	*g*	20	17	23
Peak lateral acc head CG	*g*	36	25	47
Peak lat displ head CG wrt sled	mm	*206	185	226
Peak flexion angle	deg	*68.6	62	75
Peak twist angle	deg	68.6	62	75

* modified by Tarriere

Ewing et al. (1977) conducted full scale sled tests at the Naval Biodynamics Laboratory (NBDL) in New Orleans. Male volunteers were exposed to short duration accelerations in frontal, lateral and oblique direction. They were seated upright in a rigid chair, which was mounted in the three different directions on a HYGE accelerator. The mean peak sled acceleration was set to 7.2*g*, and the acceleration pulse is shown in Figure 2.9.

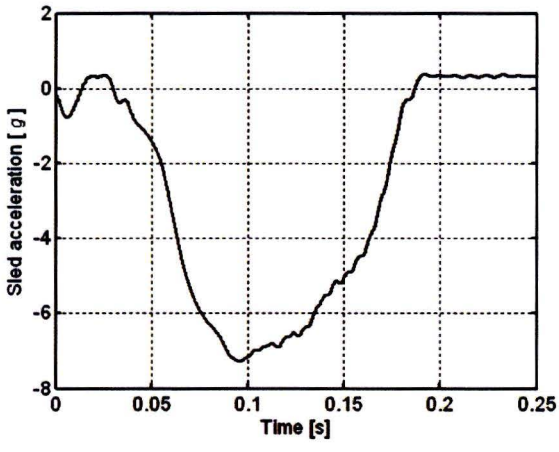

Figure 2.9: HYGE sled acceleration profile (ISO TR 9790)

Figure 2.10 Maximum head excursion in a lateral NBDL test (Ewing et al., 1978)

During the testing, all volunteers were well restrained by shoulder straps and a lap belt. To this lap belt an inverted-V pelvis strap was attached. A lightly padded wooden board was placed next to the subject to support the torso during the motion of the sled and to prevent the torso from rotating. In some cases the wrists were restrained too. The subjects were equipped with accelerometers attached to the head and to T1. Retro-reflective targets were mounted to the sled and on the volunteers as can be seen in Figure 2.10. Using cameras and these targets, the three dimensional motions of the head-neck system were monitored and analysed. The volunteers were asked to relax prior to the test.

The coordinate systems and locations of T1 and the head as defined by NBDL, as well as the locations of the head center of gravity (CG) and the OC, are shown in Figure 2.11. Both coordinate systems are orthogonal and right-handed. Head displacements were measured relative to the T1 anatomical coordinate system. The head flexion is defined as the angle in the plane of impact between the *z*-axis of the head anatomical coordinate system and the T1 coordinate system. The twist angle is the rotation of the head around the head anatomical *z*-axis.

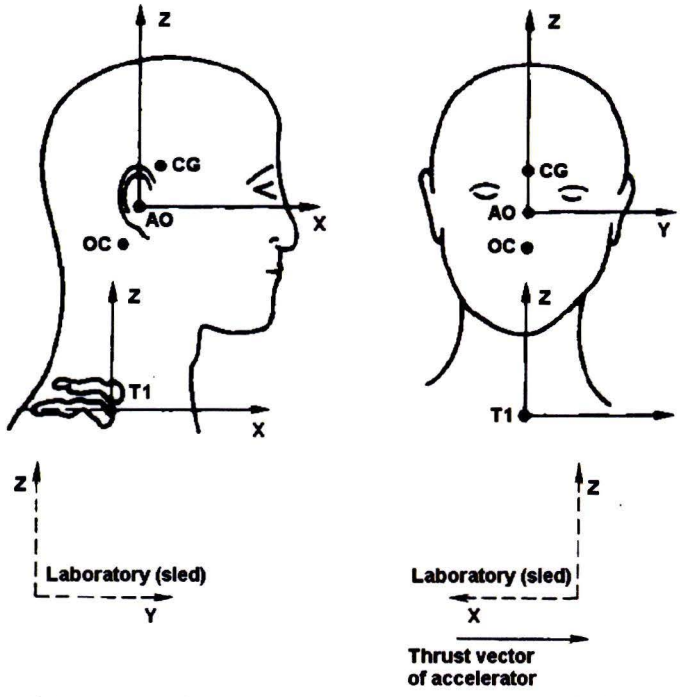

Figure 2.11: Location of the anatomical coordinate systems and orientation of the laboratory and sled coordinate systems in lateral tests according to NBDL (Wismans and Spenny, 1983)

The first volunteer tests in the lateral NBDL setup conducted by Ewing et al. (1977) were evaluated by Wismans and Spenny (1983). For these specific tests, requirements for the head-neck motion were presented. Since the torso-restraint system interaction varied considerably between different human subjects, a new test procedure for testing mechanical necks was proposed. The head-neck assembly could be tested separately from the rest of the dummy body. The T1 response of the volunteers showed that the horizontal translation is the only significant motion of the torso; rotations of T1 are found to be small enough to be neglected. Since the T1 motion can be seen as the input to the head-neck system, the base of a mechanical neck, representing T1, can be connected to and decelerated on a horizontally translating rigid structure to evaluate the dummy head response.

A new test program in the NBDL setup, which, after omission of the unusable tests, consisted of 46 frontal, 31 lateral and 32 oblique tests with 15 male human subjects, was done by Wismans et al. (1986). The head-neck responses of the volunteers were measured to define response requirements for a mechanical head-neck system for these directions.

The accelerations and displacements of T1 were analysed thoroughly. Again the only significant linear displacement of T1 was the displacement in the direction of impact and the rotations of T1 were small enough to be neglected.

The study by Wismans et al. (1986) resulted in omni-directional dummy head-neck response requirements defined relative to a non-rotating T1 coordinate system. The average peak responses of the volunteers in the lateral tests, plus or minus one standard deviation, were integrated into the ISO TR 9790 and are presented in Table 2.3.

Table 2.3 Lateral NBDL head-neck response requirements 50th male (ISO TR 9790)

Requirements		50th Male	
	Unit	Lower	Upper
Peak horizontal acc T1	*g*	12	18
Peak hor. displ. T1 wrt sled	mm	46	63
Peak hor. displ. head CG wrt T1	mm	130	162
Peak vert. displ. head CG wrt T1	mm	64	94
Time of max head excursion	s	0.159	0.175
Peak lateral acc head CG	*g*	8	11
Peak vertical acc head CG	*g*	8	10
Peak flexion angle	deg	44	59
Peak twist angle	deg	45	32

2.2.4 Biofidelity rating

To quantify the biofidelity performance of lateral dummies, an overall biofidelity rating method is presented in ISO TR 9790. Weight factors are defined for several body regions as well as for every available lateral response test to assess the biofidelity of corresponding regions. Certain boundaries for the responses, like the peak response requirements for the head-neck system in the tests described in the previous section, are also defined for these body regions. The overall biofidelity rating can vary between 0 (worst) and 10 (best). It is defined by:

$$B_i = \frac{\sum_j V_{i,j}\left(\sum_k \left(W_{i,j,k} R_{i,j,k}\right) / \sum_k W_k\right)}{\sum_j V_{i,j}}, \qquad 2\text{-}1$$

with:

B_i Biofidelity rating for a body region.
$V_{i,j}$ Weighting factor for each test condition for a given body region.
$W_{i,j,k}$ Weighting factor for each response measurement for which a requirement is given
$R_{i,j,k}$ Rating of how well a given response meets its requirement.
i Index denoting the body region (1 = head, 2 = neck).
j Index denoting the test condition for a given body region, i.
k Index denoting the response measurement for a given test condition, j and body region, i.

For R, three values can de distinguished, as presented in Figure 2.12:

$R = 10$ Response meets requirement.
$R = 5$ Response is outside requirement, but within one corridor width, cw, from the requirement.
$R = 0$ Neither of the above is met.

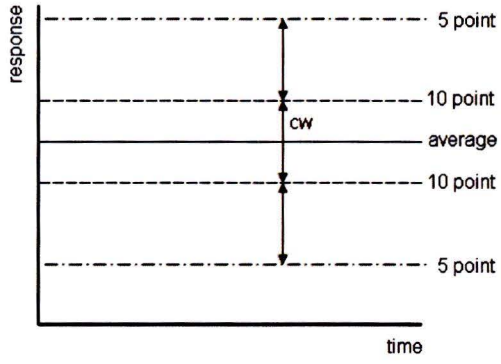

Figure 2.12 10 and 5 point boundaries to determine the rating R of peak responses

For the midsize male in the lateral NBDL test, the weight factors and boundary values are presented in Table 2.4 (ISO TR 9790). The weight factors indicate the importance of the responses relative to each other. With a weight factor of 8, the peak horizontal displacement of the head CG relative to T1 is the most important head response.

Table 2.4 Biofidelity score: reference values (ISO TR 9790)

Lateral NBDL test $V_{2,1} = 7$		**Weight factor**	**10 point boundary**		**5 point boundary**	
Response		$W_{1,2,k}$	Lower	Upper	Lower	Upper
Peak horizontal acc T1	*g*	5	12	18	6	24
Peak hor. displ. T1 wrt sled	mm	5	46	63	29	80
Peak hor. displ. head CG wrt T1	mm	8	130	162	98	194
Peak vert. displ. head CG wrt T1	mm	6	64	94	34	124
Time of max head excursion	s	5	0.159	0.175	0.134	0.191
Peak lateral acc head CG	*g*	5	8	11	5	14
Peak vertical acc head CG	*g*	5	8	10	6	12
Peak flexion angle	deg	7	44	59	29	74
Peak twist angle	deg	4	32	45	19	58

There are five classifications to indicate the degree of biofidelity:

Excellent biofidelity: $8.6 \leq B < 10.0$
Good biofidelity: $6.5 \leq B < 8.6$
Fair biofidelity: $4.4 \leq B < 6.5$
Marginal biofidelity: $2.6 \leq B < 4.4$
Unacceptable biofidelity: $0.0 \leq B < 2.6$

2.2.5 Head-neck biofidelity of 50th male WorldSID

The tests in ISO TR 9790 and the matching requirements form the base for assessment of the head-neck biofidelity of the 50th WS (Been et al. 2004). The 50th WS was tested in the lateral NBDL test setup, as shown in Figure 2.13. The black balls are retro-reflective targets mounted on the dummy and sled to define the coordinate system of the sled and dummy and to evaluate their kinematics after the test.

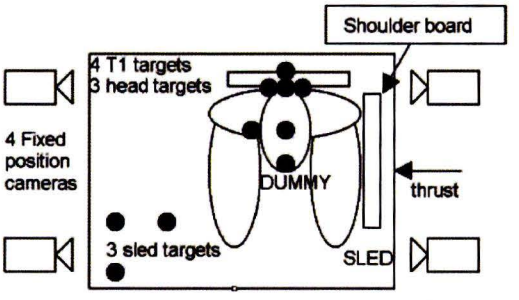

Figure 2.13 Top view of the lateral test condition (Been et al., 2004)

The average response of the three runs that were performed in this setup as well as the corresponding response requirements are presented in Table 2.5. It was found that only the head displacements and angles are situated inside the five point boundaries, the rest of the peak responses meet the ten point requirements.

Table 2.5 Requirements and responses for the head-neck system of 50th WS (Been et al., 2004)

		50th Male Requirements		50th WS
Response		Lower	Upper	
Peak horizontal acc T1	*g*	12	18	12.3
Peak hor. displ. T1 wrt sled	mm	46	63	46.7
Peak hor. displ. head CG wrt T1	mm	130	162	126.3
Peak vert. displ. head CG wrt T1	mm	64	94	59.7
Time of max head excursion	s	0.159	0.175	0.171
Peak lateral acc head CG	*g*	8	11	10.7
Peak vertical acc head CG	*g*	8	10	9.9
Peak flexion angle	deg	44	59	61
Peak twist angle	deg	45	32	20

These responses result in a biofidelity score of 7.5 for the NBDL test setup, which means that the biofidelity of the head-neck system of the 50th male WS is good. The biofidelity scores for Patrick and Chou, and Tarriere are respectively 2.4 and 6.1.

When analyzing the biofidelity scores it can be stated that the Tarriere values are fair, the NBDL values are good and the Patrick and Chou values are unacceptable. This means that the Patrick and Chou requirements are not very compatible with those of NBDL and Tarriere. Considering that they are based on one single test, their importance can be questioned.

Overall, it can be stated that the head-neck system of the 50th WS has 'good' biofidelity according to the results of the sled tests in the lateral NBDL setup.

2.3 5th female WorldSID

2.3.1 History

After developing a 50th male WorldSID the focus was shifted to the small female who represents a part of the population (small females and male and female adolescents) that is often at highest risk in crash scenarios (Barnes et al., 2005). One of the goals of the APROSYS consortium is to develop a small, also called 5th percentile, female WorldSID (5th WS) which has the same level of functionality and equal injury assessment capabilities as the 50th WS. Here, with 5th percentile female dummy is meant that only 5 percent of the female population has a smaller length and only 5 percent has a smaller weight than this dummy.

The anthropometry of the 5th WS is based on the small female anthropometry from the database of Schneider et al. (1983). This database was also used to develop the 50th WS. Table 2.6 shows the anthropometry of both the small female and the midsize male.

Table 2.6 Standard size anthropometry (Schneider et al., 1983)

Description	Units	Small Female	Mid Male
Standing height	mm	1513	1751
Erect sitting height	mm	812	907
Head circumference	mm	534	574
Head width	mm	145	154
Head depth	mm	183	197
Neck circumference	mm	304	383
Head mass	kg	3.67	4.54
Neck mass	kg	0.77	1.54
Total body mass	kg	46.72	78.20

The head and neck of the 5th WS were designed similar to the 50th WS, except that the geometry, mass and mechanical properties of the 5th female were used.

For validation of the responses of a 5th female dummy in side impact, it would be most biofidelic to define response requirements from side impact tests with small female subjects. However, such side impact test data are not available. Therefore, the response requirements for the midsize male were scaled for a small female. Currently, the response requirements were scaled according to the method of Irwin et al. (2002).

2.3.2 Scaling of responses

Scaling of geometry and responses is called geometric scaling if all length dimensions scale with the same factor. In non-geometric scaling, x-, y- and z-dimensions scale with different scaling factors.

For both geometric and non-geometric scaling, the standard way to calculate a scale factor λ for a certain dimension j is:

$$\lambda_j = \frac{l_i}{l_s}, \qquad 2\text{-}2$$

where l_i is in this case the length of target subject i and l_s is the length of the standard subject s. Normally, the standard subject is a midsize male. The lengths of the target subject and the standard subjects can be found in an anthropometry database, in the case of the WorldSID dummies in Schneider et al. (1983). Over the years quite some research on scaling has been done. Below, the most generally accepted scaling methods in biomechanics are described.

2.3.3 Scaling method of Mertz

Mertz (1984) presented a procedure for normalizing impact response data, using the lateral thoracic impact of cadaver specimens as an example, of various sizes of test subjects to define the responses of a standard size specimen, in this case the midsize male. This was done by defining a relationship between the appropriate physical characteristics, the impact test parameters and the response. Using this approach and the response requirements for the Hybrid III, a midsize male frontal dummy, frontal impact biofidelity requirements were defined for a small adult female and a large adult male (Mertz et al., 1989).

From the anthropometry database of Schneider et al. (1983) the key body segments lengths and weights, on which the scale factors are based, are selected. These factors are defined to assure that the mass density of each body segment is the same as for the corresponding segment of the Hybrid III. In every database the body segment weights are estimated from the length measurements and a particular way of dividing the body in different sections, a sectioning scheme. The mass of the segments for the two new dummies had to be calculated, for the body sectioning scheme of Schneider et al. (1983) is not the same as the one used for the Hybrid III dummy.

These constraints of equal density and unknown weights lead to the assumption that the head geometry is considered to be a sphere and is scaled by a characteristic length factor:

$$\lambda_{x\,head} = \lambda_{y\,head} = \lambda_{z\,head} = \frac{(C+W+H)_i}{(C+W+H)_{midmale}}, \qquad 2\text{-}3$$

where C is the head circumference, W the head width and H the head height.

For geometrically similar objects with equal density, the mass scale ratio λ_m can be calculated by taking the 3rd power of the characteristic length. For the head this leads to:

$$\lambda_{m\,head} = (\lambda_{x\,head})^3 . \qquad 2\text{-}4$$

The erect sitting height (*ESH*) is used as the characteristic length in the *z*-direction for both neck and torso:

$$\lambda_{z\,neck} = \frac{ESH_i}{ESH_{midmale}} . \qquad 2\text{-}5$$

The scale factor for the mass of the neck $\lambda_{m\,neck}$ is defined as:

$$\lambda_{m\,neck} = \frac{TBM_i}{TBM_{midmale}} , \qquad 2\text{-}6$$

where *TBM* is the total body mass. The neck is considered to be a cylinder. To maintain equal density the *x*- and *y*-scale factors of the neck, $\lambda_{x\,neck}$ and $\lambda_{y\,neck}$, are assumed to be equal:

$$\lambda_{x\,neck} = \lambda_{y\,neck} = \sqrt{\frac{\lambda_m}{\lambda_{z\,neck}}} . \qquad 2\text{-}7$$

A method to scale the head-neck response for tests in the frontal NBDL setup was not defined in Mertz et al. (1989). Only some general response scaling equations for the head and neck were discussed briefly.

2.3.4 Scaling method of Irwin

Irwin et al. (2002) developed guidelines for assessing the biofidelity of side impact dummies. The anthropometry database of Schneider et al. (1983) was also used in this study to define scale factors for different parameters. The anthropometry of the small female and midsize male is shown in Table 2.6.

In the following section, only the scaling equations and their origin are presented briefly. An extensive derivation of the scaling equations of Irwin et al. is presented in appendix A.

The head lengths and head mass scale like equation 2.3 and 2.4. With these scale factors, the scale factor for the moment of inertia of the head $\lambda_{Iz\,head}$ can be defined as:

$$\lambda_{Iz\,head} = \lambda_{m\,head}(\lambda_{x\,head})^2. \qquad 2\text{-}8$$

In the study of Irwin, the neck is scaled in a different way than before. Defining injury risk curves, Mertz et al. (1997) assumed the neck of humans of different age and geometry to be geometrically similar and all dimensions are proportional to the neck circumference. Equal density is still assumed, so the neck mass is slightly different from that of the Hybrid III dummy. The geometrical scale factor for the neck λ_{neck} is defined as:

$$\lambda_{x\,neck} = \lambda_{y\,neck} = \lambda_{z\,neck} = \frac{(NC)_i}{(NC)_{midmale}}, \qquad 2\text{-}9$$

where NC is the neck circumference. The mass scale factor of the neck, $\lambda_{m\,neck}$, is given as:

$$\lambda_{m\,neck} = (\lambda_{x\,neck})^3. \qquad 2\text{-}10$$

The elastic modulus E of either bone or soft tissue is scaled as follows:

$$\lambda_{E\,j} = \frac{E_{j\,i}}{E_{j\,midmale}}, \qquad 2\text{-}11$$

where E is the elastic modulus and j represents bone or soft tissue. Since there is no difference between the elastic modulus of either bone or soft tissue of different sized adults, the scale factor is one.

With respect to lateral sled tests it is useful to calculate two stiffness ratios for the neck: the bending stiffness and the twist stiffness. To calculate the bending stiffness, the neck is assumed to behave like a cantilever beam, shown in Figure 2.14. The angle ϕ and displacement u of the free end of a cantilever are calculated as described by Fenner (1989).

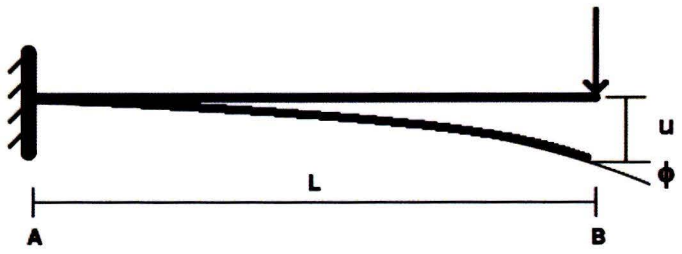

Figure 2.14 Cantilever beam

The stiffness of a cantilever beam is the basis of the scale factor for the neck bending stiffness of the neck:

$$\lambda_{k\,Mx\,neck} = \lambda_{E\,soft}\frac{(\lambda_{y\,neck})^4}{(\lambda_{z\,neck})^3} = \lambda_{E\,soft}\lambda_{y\,neck}. \qquad 2\text{-}12$$

Note here that λ_{Esoft} equals 1 and therefore could be omitted. The equation for torque T of a cylindrical shaped beam around its length axis (Fenner, 1989) is the basis to derive the scale factor for twist of the neck around its z-axis $\lambda_{k\,Mz\,neck}$:

$$\lambda_{k\,Mz\,neck} = \lambda_{G\,neck}\frac{(\lambda_{y\,neck})^4}{\lambda_{z\,neck}} = \lambda_{G\,neck}(\lambda_{y\,neck})^3. \qquad 2\text{-}13$$

Here, λ_{Gneck} is the scale factor for the torsional modulus, which is equal to the shear modulus. It is calculated in the standard way and set to one since the torsional modulus of the neck is based on the elasticity of soft tissue:

$$\lambda_{G\,neck} = \frac{G_{neck\,i}}{G_{neck\,midmale}}. \qquad 2\text{-}14$$

To calculate the lateral flexion angle, the head-neck system is modeled as a spring, having the properties of a cantilever beam, with a point mass on it. They represent the neck and the head mass respectively, as displayed in Figure 2.15. The response scale factors are denoted by R. The kinetic energy of the system is converted to elastic energy of the spring, which leads to the following scale factor for the neck bending angle R_ϕ:

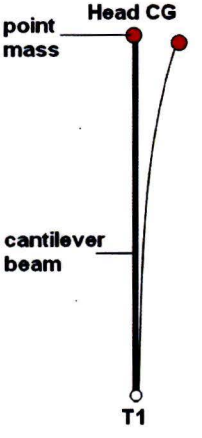

Figure 2.15
Mass-spring representation of the head-neck system

$$R_\phi = \frac{\lambda_v}{\lambda_{z\,neck}}\sqrt{\frac{\lambda_{m\,head}}{\lambda_{k\,Mx}}}, \qquad 2\text{-}15$$

where λ_v is the velocity scale factor. It is calculated in the standard way (see equation 2-2) and also set to one, since no difference in velocity is present. To derive the scale factor for the twist angle of the neck, the same principle as for the bending angle applies, though adjusted to the direction. The following scale factor for the twist angle is derived:

$$R_\theta = \frac{\lambda_v}{\lambda_{x\,head}}\sqrt{\frac{\lambda_{Iz}}{\lambda_{k\,Mz}}}. \qquad 2\text{-}16$$

In the following passage, the approach for deriving the peak lateral and vertical head displacement is described, where $u_{midmale}$ is the peak head displacement of the midsize male, as displayed in Figure 2.16, and it is derived as:

$$u = \sqrt{\delta_y^2 + \delta_z^2} \,. \qquad 2\text{-}17$$

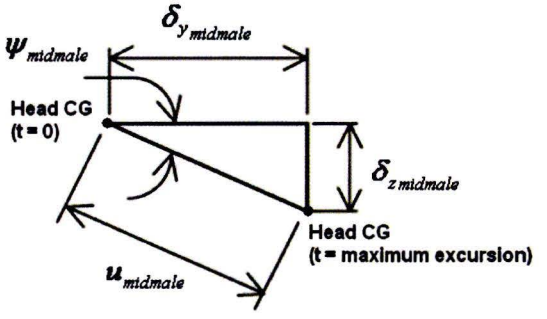

Figure 2.16 Dimensions used to calculate peak head displacements (Irwin et al., 2002)

The scale factor for this displacement R_u is:

$$R_u = \lambda_v \sqrt{\frac{\lambda_{m\,head}}{\lambda_{k\,Mx}}} \,. \qquad 2\text{-}18$$

The angle $\psi_{midmale}$ is scaled by equation 2-15.

To calculate the peak displacements of the head, first the angle ψ_i and scaled displacement u_i need to be calculated. Using these dimensions the peak displacements of the head in lateral δ_{yi} and vertical δ_{zi} direction are calculated:

$$\psi_i = R_\phi \psi_{midmale}\,, \qquad 2\text{-}19$$

$$u_i = R_u u_{midmale}\,, \qquad 2\text{-}20$$

$$\delta_{yi} = u_i \cos(\psi_i)\,, \qquad 2\text{-}21$$

$$\delta_{zi} = u_i \sin(\psi_i)\,. \qquad 2\text{-}22$$

The scale factor for the maximum head excursion period is defined as:

$$R_{th} = \sqrt{\frac{\lambda_{m\,head}}{\lambda_{k\,Mx}}} \,. \qquad 2\text{-}23$$

The acceleration ratio in lateral direction R_{ahy} is based on the standard relations of a mass spring model (Mertz et al., 1989):

$$R_{ahy} = \lambda_v \sqrt{\frac{\lambda_{k\,Mx}}{\lambda_{m\,head}}}. \qquad 2\text{-}24$$

The vertical non impact acceleration scale factor of the head (R_{ahz}) is calculated as:

$$R_{ahz} = \frac{(\lambda_v)^2}{\lambda_{z\,neck}}. \qquad 2\text{-}25$$

2.3.5 Head-neck response of 5th female WorldSID prototype

The small female WorldSID (5th WS) prototype has been developed by scaling down the average male WorldSID according to the anthropometry database of Schneider et al. (1983). The lateral biofidelity of the head-neck system is assessed according to the neck tests described in ISO TR 9790. The requirements which the peak values should meet, are defined by Irwin et al. (2002) and given in Table 2.7.

As already stated in section 2.2.5, the requirements of Patrick and Chou are based on only one test. No requirement for the acceleration or displacement of T1 is described either, which makes it impossible to compare the 5th WS T1 response with the T1 response requirement of Patrick and Chou. Since the T1 response is the input to the head-neck system, the head kinematics and dynamics of the 5th WS cannot be compared to the requirements of Patrick and Chou. Therefore, these requirements are left out of the biofidelity assessment of the 5th WS (Meijer et al., 2007).

No scaling equation for the required peak horizontal displacement of the head CG relative to the sled was presented in Irwin et al. (2002). Since this is the most important parameter of the Tarriere requirements, its loss reduces the relevance of this test. Therefore, the 5th WS is not tested in the Tarriere setup (Barnes et al., 2005).

Summarising, this means that the 5th WS is only tested in a lateral NBDL test setup to evaluate the biofidelity of the head-neck system.

A prototype of the 5th WS has been developed and tested in the lateral NBDL test setup. Irwin et al. defined head-neck response requirements for the lateral NBDL test using the equations presented in section 2.3.4 in combination with data from the anthropometry database of Schneider et al. (1983). Table 2.7 shows the head-neck response requirements for the midsize male and small female in a lateral NBDL test setup as well as the peak responses of the 5th WS prototype.

Table 2.7 Head-neck response requirements according to Irwin et al. (2002)

		Requirements 50th Male		Requirements 5th Female (Irwin)		Test 5th WS
Response		Lower	Upper	Lower	Upper	
Peak horizontal acc T1	*g*	12	18	15	22	10.0
Peak hor. displ. T1 wrt sled	mm	46	63	38	51	28.1
Peak hor. displ. head CG wrt T1	mm	130	162	121	151	108.2
Peak vert. displ. head CG wrt T1	mm	64	94	80	118	56.0
Time of max head excursion	s	0.159	0.175	0.161	0.177	0.158
Peak lateral acc head CG	*g*	8	11	8	11	10.1
Peak vertical acc head CG	*g*	8	10	10	13	9.4
Peak flexion angle	deg	44	59	56	75	66
Peak twist angle	deg	45	32	57	41	13

Figure 2.17 to Figure 2.24 show the responses of the head-neck system in time as well as the corresponding peak response corridors (red) for the peak values defined according to Irwin.

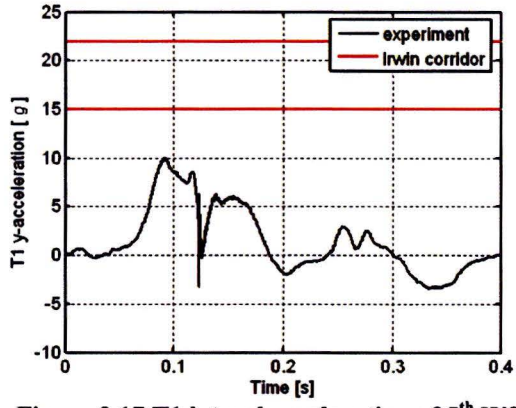

Figure 2.17 T1 lateral acceleration of 5th WS prototype (Meijer et al., 2007)

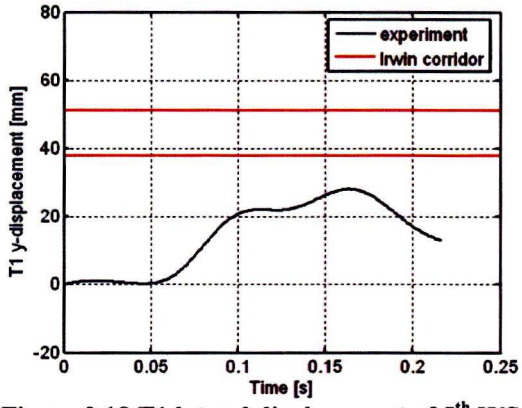

Figure 2.18 T1 lateral displacement of 5th WS prototype (Meijer et al., 2007)

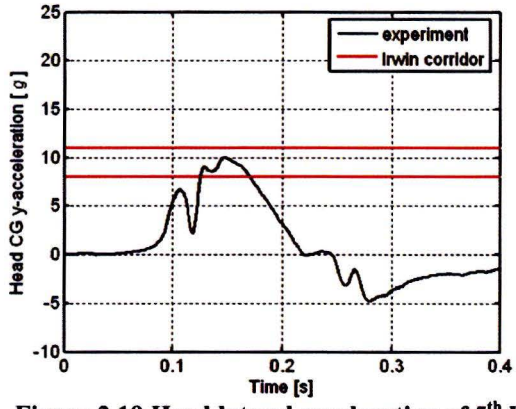

Figure 2.19 Head lateral acceleration of 5th WS prototype (Meijer et al., 2007)

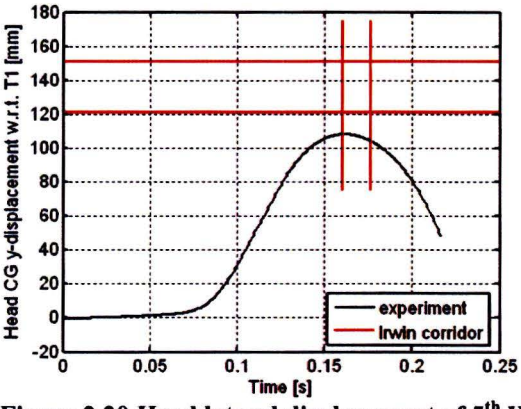

Figure 2.20 Head lateral displacement of 5th WS prototype (Meijer et al., 2007)

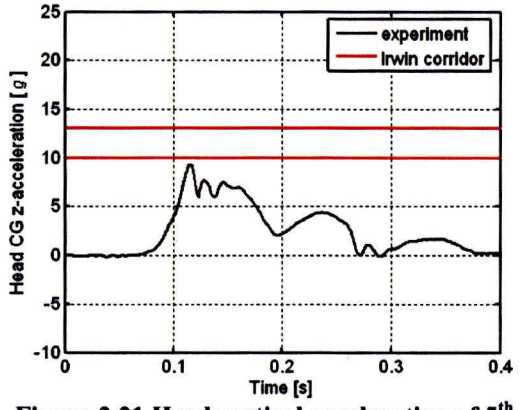

Figure 2.21 Head vertical acceleration of 5th WS prototype (Meijer et al., 2007)

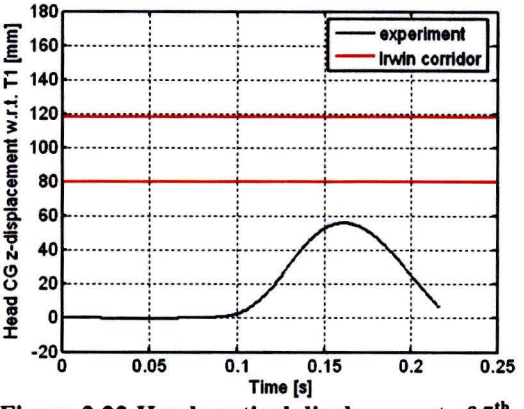

Figure 2.22 Head vertical displacement of 5th WS prototype (Meijer et al., 2007)

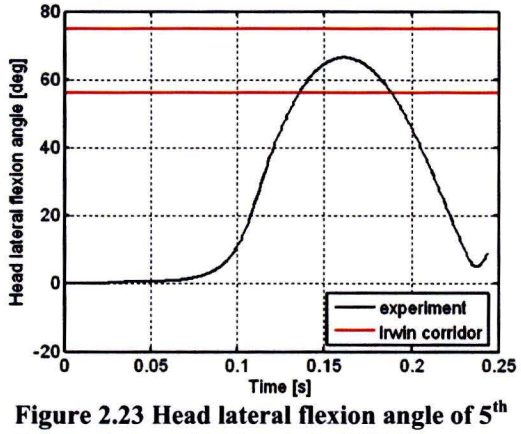

Figure 2.23 Head lateral flexion angle of 5th WS prototype (Meijer et al., 2007)

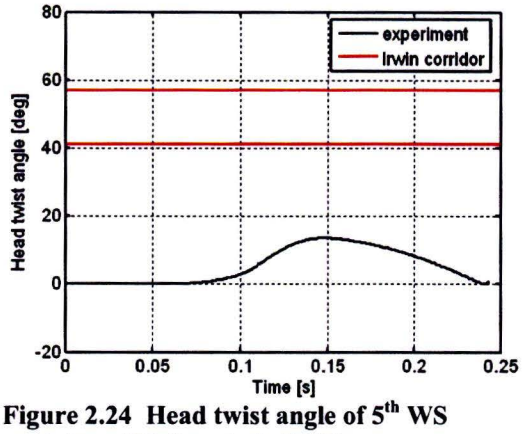

Figure 2.24 Head twist angle of 5th WS prototype (Meijer et al., 2007)

As can be seen in Figure 2.17 and Figure 2.18 the T1 peak responses do not meet the requirements. This means that the input to the head-neck system of the dummy is not biofidelic. The shoulder of the 5th WS is probably too stiff.

The lateral acceleration of the head, shown in Figure 2.19 met the requirements and the vertical acceleration, shown in Figure 2.20 is within 1*g* from the requirements. However, the lateral as well as the vertical displacements of the head was too low, as shown in Figure 2.22 and Figure 2.20, respectively. This is logical since the T1 response was also too low. The timing of the maximum displacement was satisfactory though. The head flexion was well inside the peak response corridor as can be seen in Figure 2.23, which should not be the case for this T1 response. The peak head twist was far too small as displayed in Figure 2.24. This is also the case for the 50th WS, see section 2.2.5. This is caused by the special buffers in the dummy neck design which provide extra torsional stiffness (Been et al, 2004). These buffers were also present in the head-neck system of the 5th WS prototype.

3. Scaling analysis

3.1 Methodology

The first objective of this study is to analyse the head-neck scaling method proposed by Irwin et al. to provide a judgement on its validity. Therefore, research was done to find the gender-related differences relevant to head-neck scaling, as can be read in section 3.2. The general model of the head-neck system that Irwin proposes and the corresponding assumptions that were made to develop this head-neck scaling method are discussed in section 3.3. These assumptions were compared to the differences between males and females, as stated in literature. After that, relations are to be found between anthropometry of the head-neck and the corresponding responses, as described in section 3.4. For this, the male volunteers of the NBDL tests and their peak responses have been used. In section 3.5, the results of this analysis were compared to the scaling method for the head-neck system, proposed by Irwin, to give a clear judgement on the validity of the scaling. Thereafter, a new scaling method was developed and new response requirements were proposed.

3.2 Gender-related differences relevant to head-neck scaling

3.2.1 Anthropometry

It is clear that males and females differ in anthropometry. Generally, all linear body dimensions of males are larger than those of females, except the hip breadth is proportionally wider in females. The arms and legs are proportionally and absolutely larger in males (Mordaka, 2004). Therefore, the ratio of sitting height to stature will be greater in females than in males. In general, females also have a smaller body mass than males. With respect to the head-neck system, it can be stated that, compared to males, females have a smaller head both in geometry as well as in mass. Schneider et al. (1983) present a ratio of 0.81 between a small female and a midsize male head. In the database People Size (1998) a ratio of 0.94 is found for the head breadth of 50th percentile males and females. For the head length this ratio is 0.92. It has also been reported that the neck cross-section and circumference of females is smaller than that of males, as presented in Table 3.1. The ratio of circumferences is 0.83-0.93.

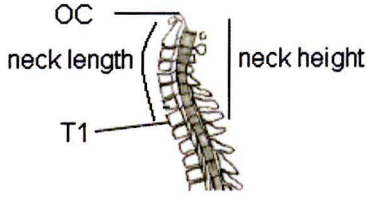

Figure 3.1 Neck length and height (www.neurosurgeon.org)

Other important neck parameters are the neck length and height. The neck height is defined as the distance between the occipital condyles and the last (seventh) cervical vertebra (C7) and the length is reported as the length of the cervical lordosis as displayed in Figure 3.1. This is the curvature of the neck. Table 3.1 shows the differences in the neck section between males and females.

Table 3.1 Neck related measurements (Mordaka, 2004)

Parameter	Female		Male		Female / Male
	Mean [mm]	SD [mm]	Mean [mm]	SD [mm]	Ratio
Neck circumference (Harty, 2004)	342	2.3	409	3.6	0.83
Neck circumference (Vasavada, 2001)	360	20.0	390	20.0	0.93
Neck circumference (People Size, 1998)	373	26.4	399	25.7	0.93
Neck height* (Valkeinen,2003)	64		62		1.03
Neck length* (Harty, 2004)	124	18.0	125	175.0	0.99
Height** / Length ratio*** (Harrison, 1996)	97.00%	1.5	96.95%	1.6	

* Occiput-C7 spinous process

** Height was defined as length of chord of cervical lordosis

*** Length was defined the length of arc of cervical lordosis arc

From these data it can be concluded that, in general, the difference in neck circumference between males and females is larger than the difference in neck height and length.

3.2.2 Head-neck response

Schneider et al. (1975) measured anthropometry and responses of 96 both male and female volunteers of different age and size. The anthropometric values of the head, the neck and the whole body were measured as well as a couple of responses of the head-neck system:

- three dimensional range of motion
- response to low level acceleration
- reflex time
- voluntary isometric muscle force in lateral direction

The ranges of motion in lateral bending, also called lateral flexion, of young male and female subjects were found to be similar. However, the range of motion decreases with age for both males and females, but faster for males, as given in Table 3.2. This table also includes the rotation of the head-neck system around its vertical axis.

Table 3.2 Range of motion per sex and age category (Schneider et al., 1975)

Subjects	Range of motion [degrees]			
	Lateral bending		Rotation	
Age	Male	Female	Male	Female
18 - 24	86.3	86.0	149.5	150.6
35 - 44	73.0	73.9	137.1	143.6
62 - 74	48.0	56.3	113.9	123.6
All	69.8	72.0	133.7	139.3
All of both sexes	71.0		136.5	

In a voluntary head-pulling test, males show 1.5 to 2 times greater strength in the neck muscles than females and for both sexes the strength decreases with age. Reflex times to lateral head loading range from 30 to 70 ms and are smaller for females than for males. These differences may not be significant in complete surprise impact as the total time to maximum muscle force, including 100 ms contraction time, is in the order of 130-170 ms. This is probably too long to prevent injury in high-speed collision.

Youdas et al. (1992) measured the head and neck range of motion of 171 females and 166 males with ages ranging from 11 to 97 years. The difference between males and females for both the range of motion of the neck rotation about its length axis as well as the range of motion in lateral bending was two to three degrees. This study also showed that the range of motion decreased with age.

Tilley (1993) found a range of motion in lateral bending of 54 degrees to either side for both males and females. He also stated that there is no difference in this range of motion between males and females of different body size.

Vasavada et al. (2001) measured the maximum flexion, extension, lateral bending and axial rotation moments in 11 males and 5 females subjects (aged 20-42). The lateral bending moment measured on the male subjects was approximately two times larger than the moment measured on the females. Table 3.3 provides a comparison of these results to those of other studies.

Table 3.3 Results of several studies on neck moments

Reference	No of subjects	Gender	Point of moment resolution	Flexion moment [Nm]	Extension moment [Nm]	Lateral bending moment [Nm]	Axial rotation moment [Nm]
Choi and Vanderby (1999)	10	M	C4 - C5	18±3	28±3	17±3	-
Moroney et al. (1988)	10	M	C4 - C5	12±7	30±15	15±8	10±3
	4	F	C4 - C5	6±3	17±7	8±4	6±2
Vasavada et al. (2001)	11	M	C4	30±5	52±11	36±8	15±4
			C7 -T1	19±4	35±8	25±6	14±4
			Mastoid	13±3	24±7	17±5	15±4
	5	F	C4	15±4	21±12	16±8	6±3
			C7 -T1	10±2	15±8	10±5	6±3
			Mastoid	6±1	10±5	6±3	6±3

M = male
F = female

Ono et al. (2007) conducted lateral shoulder impactor tests with 5 male and 3 female volunteers in order to get insight in the response of the head, neck and torso during a lateral collision. To find differences in effects of the neck muscle response on the motion of head, neck and torso, the tests were done with and without muscle tension. For the same test conditions, without muscle tension, no difference between the peak T1 acceleration for males and females were found. However, the maximum acceleration of the head CG under these conditions was higher for females than for males. The presence of muscle tone resulted in a suppression of both the peak displacement of the head CG and the peak rotation of the head. This suppression was greater for males than for females. This shows again that males have stronger neck muscles than females. However, it was also found that under the same test conditions, males and females with relaxed muscles showed approximately the same peak head CG displacements and peak head rotations.

3.3 Scaling method of Irwin applied to the head and neck

3.3.1 Assumptions

To come to the response requirements for a 5th female head-neck system, Irwin et al. made the following assumptions:

1. The neck circumference is used to determine the scale factor of the neck in all three directions.

2. The anthropometry database of Schneider et al. (1983) is used, that is based on measurements of 13645 US citizens with an age ranging from 18 to 74 years old.

3. The head-neck system is modeled as a spring with mass on it. The spring represents the neck and the mass represents the head. To calculate the neck stiffness in bending and twist, it is assumed that the neck behaves like a cantilever beam with a circular profile.

In the next sections, these three assumptions are discussed to find out whether they are valid for the human head-neck response and if not, whether any improvements can be made to these aspects of the method of Irwin. Especially the third assumption is of major importance, because the scaling rules, corresponding to the proposed model, determine the resulting response requirements to a large extent.

3.3.2 Neck scale factor

According to Irwin only one neck scale factor for all directions is used and it is based on the neck circumference. The validity of this assumption is highly questionable. In literature about differences between males and females, presented in section 3.2, it is found that the difference in neck length between males and females is smaller than the difference in neck circumference. In addition, a neck circumference of an adult could change over the years, but a neck length does not. Therefore, it would be reasonable to separate the neck scale factor in vertical direction, z, from both scale factors in lateral direction, x and y. The x and y scale factor could still be based on the neck circumference and the scale factor for the neck length should be based on a vertical dimension. Normally, the neck length is not a parameter that is taken up in anthropometry databases, probably because it is not a standard length to measure, like for example the neck circumference. The scaling factor for the neck length could be based on the erect sitting height, as proposed by Mertz et al. (1989).

3.3.3 Anthropometry database

The database used by Irwin (Schneider et al., 1983) consists of measurements on 13645 US citizens of different age and proportion. A major shortcoming of the database is that it only consists of measurements of people in the United States. Generally, these people can be considered taller than for example Asian people. Since the WorldSID is supposed to represent the world population, it would have been better to base its geometry and response on the world population. The database People Size (1998), for example, is an anthropometric database which consists of measurements of large subsets of people from eight different countries, including, among others, Japan, the United Kingdom, Germany and the United States. In future development of dummies representing the world population, such a database should be used. Nevertheless, the question if it is realistic to develop a dummy which represents the world population will not be answered during this study, since it is out of the scope of the project.

3.3.4 Model of the head-neck system

The head-neck system is considered to be a spring-mass system, where the head is represented by a mass and the neck is modeled as a spring with the properties of a cantilever beam, as was described in section 2.3.4 and appendix A. Using this model, the response equations on which the head-neck scaling requirements of Irwin are based, are derived.

From literature on the differences in head-neck response between males and females, as presented in section 3.2.2, conclusions were drawn which are in contradiction with the assumption of Irwin to take the difference in neck stiffness into account. The stiffness of the cantilever beam is a way to model the resistance that the neck muscles of a person can deliver. Typically, males can exert a larger maximum force with their neck muscles than females can and females have shorter response times (Schneider et al., 1975; Vasavada et al., 2001). The response time plus the time it takes to reach maximum muscle force (130-170 ms) is almost as long as the time of maximum excursion of the head, measured in the NBDL volunteer tests (159-177 ms). Therefore, the differences in neck strength are not that significant in the lateral NBDL setup. The NBDL volunteers did not pretense their neck muscles previous to the impact, so it can be stated that difference in neck stiffness, due to stronger muscles, does not play a major role in the NBDL setup.

From the contradiction between literature and these assumptions of Irwin it can be concluded that this scaling method is not valid for scaling the head-neck response of the volunteers in the lateral NBDL tests.

Not all anthropometry data of the individual volunteers that are necessary to predict their head response according to Irwin, are available for the NBDL tests. Therefore, a comparison with measured peak responses in order to verify this conclusion cannot be made and another approach is chosen, which is described in section 3.4.

3.4 NBDL volunteer analysis

3.4.1 Anthropometric measures vs. responses

The lateral head-neck response requirements are based on the peak responses of the male volunteers that participated in the NBDL sled tests, see section 2.2.3. Finding a relation between the anthropometry of the head-neck system of the volunteers and their head response can lead to a new insight with respect to the expected response of small females. Since this study is about the head-neck response in side impact, relations were only sought in the side impact NBDL tests.

Anthropometric measurements were conducted for each volunteer as part of the NBDL test protocol. Among others, also the initial neck length was measured. This is the distance between the T1 and head anatomical origin just before impact (Wismans et al., 1986). The subject's head mass has been estimated based on measured head geometry data and using the regression equations proposed by McConville et al. (1980). These anthropometric values and some neck circumferences of all volunteers are presented in Table 3.4. The five measured neck circumferences are of subjects used in frontal tests (Thunnissen et al., 1995). The neck circumferences of the rest of the volunteers could not be found.

Table 3.4 NBDL Volunteer anthropometry (Wismans et al., 1986)

Subject number	Standing height [m]	Weight [kg]	Initial neck length [m]	Neck circumference [m]	Head mass [kg]
H00118	1.86	73.8	0.172		4.79
H00120	1.73	83.0	0.172		5.14
H00127	1.72	62.1	0.162	0.355	4.40
H00130	1.80	72.6	0.180		4.75
H00131	1.67	67.6	0.156	0.394	4.98
H00132	1.73	79.8	0.141	0.395	5.05
H00133	1.62	61.2	0.165	0.377	4.70
H00134	1.78	75.3	0.158		4.81
H00135	1.72	68.9	0.150	0.376	4.32
H00136	1.85	88.9	0.173		4.77
H00138	1.86	78.9	0.174		4.87
H00139	1.74	72.6	0.164		4.94
H00140	1.77	86.2	0.173		4.88
H00141	1.83	80.7	0.175		4.57
H00142	1.82	87.5	0.161		4.75
average	1.77	75.9	0.165	0.379	4.78

Four peak responses were plotted as a function of the neck length as well as the head mass: the maximum flexion of the head, the maximum twist of the head and the peak displacements of the head CG in both lateral as well as vertical direction. These peak response data were taken from the most severe sled tests in lateral direction (Wismans et al., 1986), since the head-neck response requirements were derived from these tests (ISO TR 9790).

Regression analysis was used to find relations between these anthropometry parameters and the head responses (Montgomery and Runger, 1999). The straight lines in the figures are the least squared models resulting from this linear regression analysis. More information about regression analysis can be found in appendix B. Furthermore, the coefficient of determination (R^2) and the correlation coefficient (ρ) were used to define the accuracy of the regression models. R^2 defines the amount of variability in the data explained by or accounted for by the regression model. ρ was used to address the relation between parameters and should be between -1 and 1. If ρ equals zero, it means that the two variables are independent of each other. A value between 0 and 1 indicates the level in which both variables increase together and a value between -1 and 0 indicates the level in which one variable increases as the other decreases. Table 3.5 gives an overview on how the positive values of ρ can indicate how much correlation is present according to Cohen (1988). This applies for negative values as well. In this study it is assumed that if both R^2 and ρ are larger than 0.5 a linear relation is likely.

Table 3.5 Correlation and corresponding values for ρ (Cohen, 1988)

Correlation	Positive values of ρ
Small	0.01 to 0.29
Medium	0.30 to 0.49
Large	0.50 to 1.00

3.4.2 Head response as function of initial neck length

Figure 3.2a to Figure 3.2d on the next page show the peak head responses as a function of the initial neck length. Figure 3.2a shows no clear linear relation between the initial neck length and the maximum flexion in the lateral experiments. Most flexion responses are located between 50 and 55 degrees. Below and above this cloud extreme values can be found. A similar pattern can be observed for the head twist, as shown in Figure 3.2b. The maximum lateral and vertical displacement on the other hand seem to depend on the neck length. Figure 3.2c and Figure 3.2d show that a longer neck results in a higher peak displacement of the head CG relative to T1.

Statistical analysis makes it possible to provide a more accurate judgement on the chosen linear relation. For the figures above the statistical parameters R^2 and ρ are presented in Table 3.6.

Table 3.6 Statistical values for the relation between neck length and head response

lateral response vs. neck length				
parameter	flexion	twist	lat displ	vert displ
R^2	0.05	0.00	0.77	0.55
ρ	0.22	0.04	0.88	0.74

For the lateral and vertical displacement 77% and 55% of the variance in the maximum displacements is accounted for by the model. Together with the corresponding high correlation coefficients it can be stated that linear relations exist between the head displacements and the initial neck length. The statistical values for both the flexion and the twist are low.

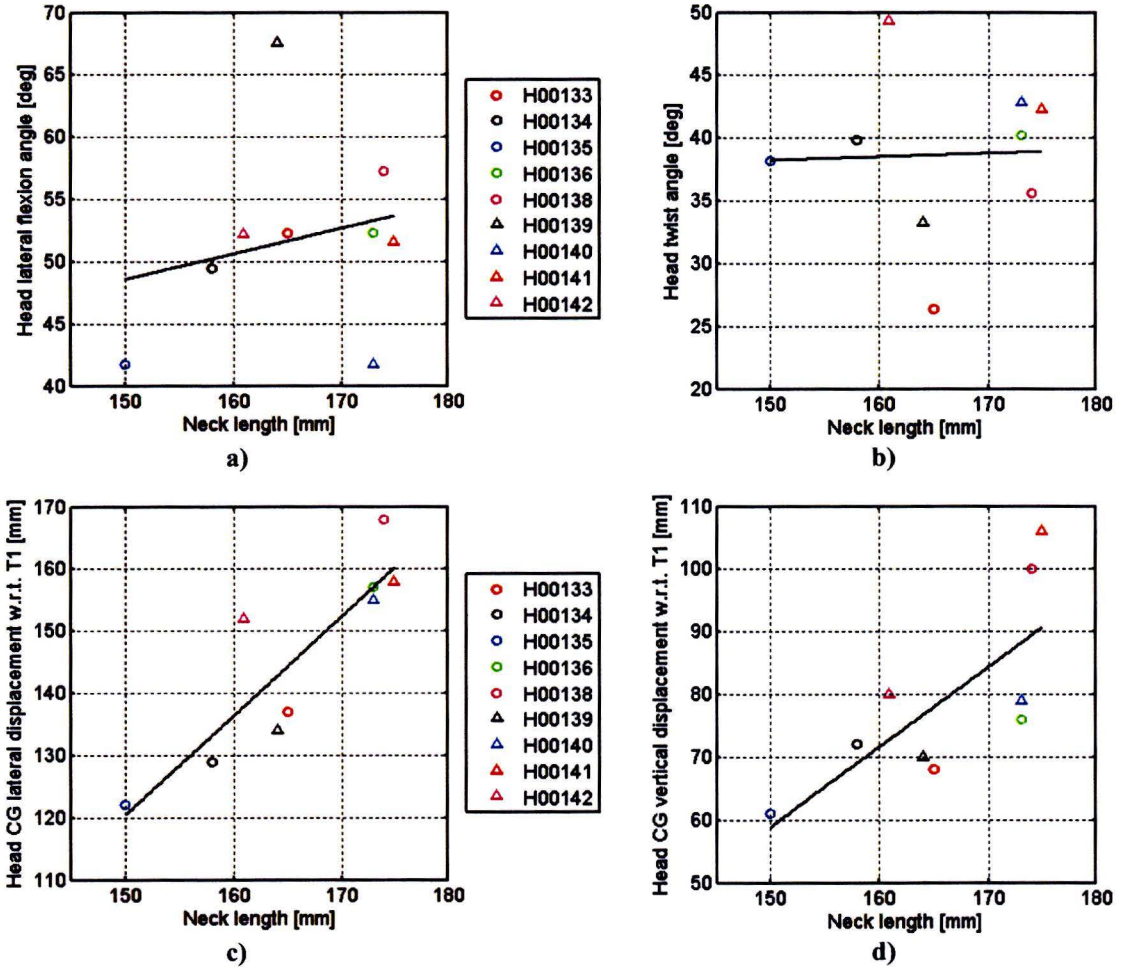

Figure 3.2 Peak lateral head flexion angle (a), peak head twist angle (b), peak lateral head displacement (c) and peak vertical head displacement (d) of the human subjects in the lateral NBDL tests vs. their neck length

3.4.3 Head response as function of head mass

Figure 3.3a to Figure 3.3d show the peak head responses as a function of the head mass.

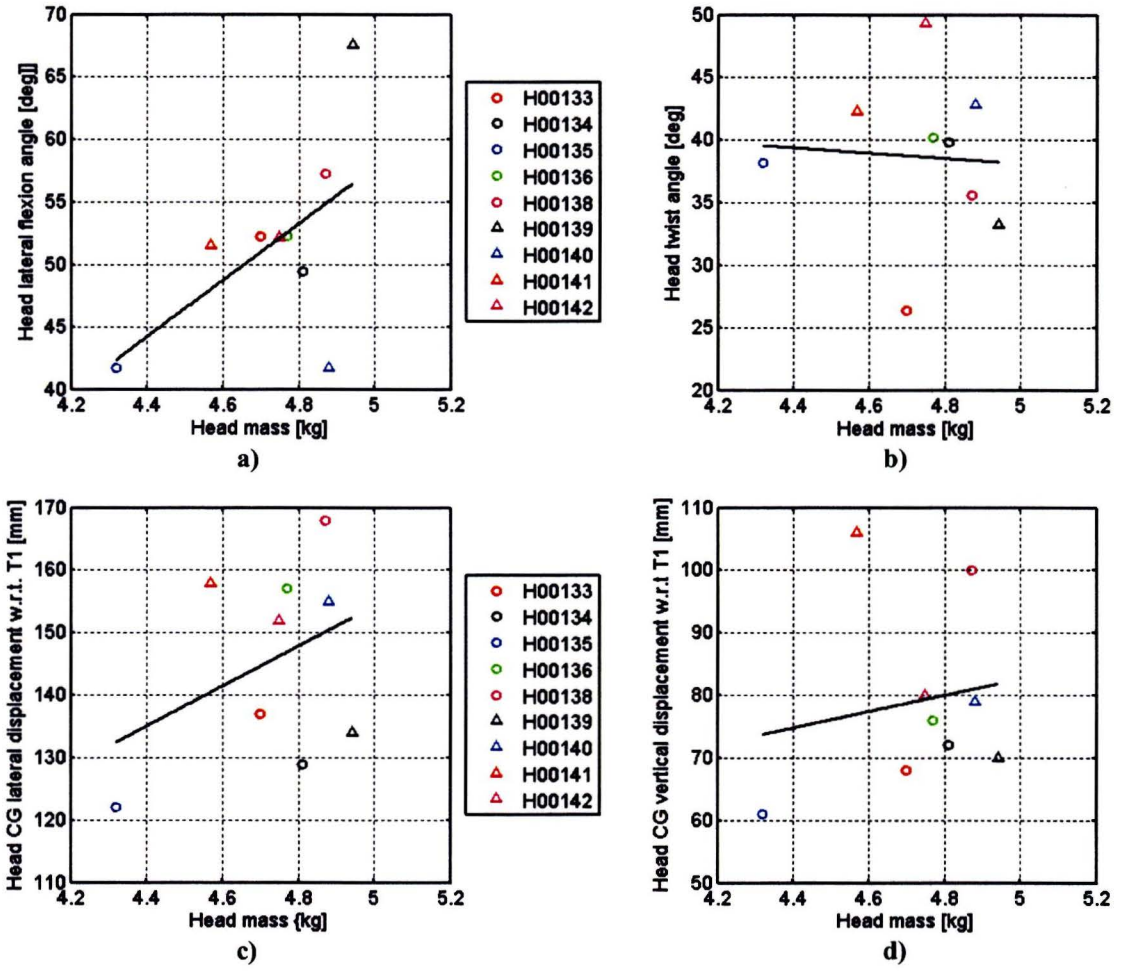

Figure 3.3 Peak lateral head flexion angle (a), peak head twist angle (b), peak lateral head displacement (c) and peak vertical head displacement (d) of the human subjects in the lateral NBDL tests vs. their head mass (ISO TR 9790)

As can be seen in the figures, the data points seem to be randomly distributed and the regression model does not account for that. A relation with respect to the head mass is hard to find. This is confirmed by the values for ρ and the R^2, given in Table 3.7, which indicate that a linear relation between the presented head responses and the head mass is not realistic.

Table 3.7 Statistical values for the relation between head mass and head response

lateral response vs. head mass				
parameter	flexion	twist	lat displ	vert displ
R^2	0.31	0.00	0.15	0.03
ρ	0.55	-0.06	0.39	0.17

3.4.4 Anthropometry parameters

A heavy head is carried by a stronger neck with stronger muscles. Therefore, the neck circumference of a person with a heavy head is expected to be larger than the neck circumference of a person with a lighter head. To investigate this, the head mass of the subjects is compared to their neck circumference. Only the neck circumferences of the human volunteer subjects used to determine the response in frontal impact can be found in literature (Thunnissen et al., 1995). Despite of the fact that there are only five neck circumferences available in literature, the comparison of these five neck circumferences with the head masses of the same human subjects shows a linear relation. The statistical parameters confirm this as shown in Table 3.8.

Table 3.8 statistical values for relations between different anthropometry parameters

parameter	head mass vs. neck circ	neck length vs. neck circ	ESH vs. neck length
R^2	0.71	0.37	0.29
ρ	0.84	-0.61	0.54

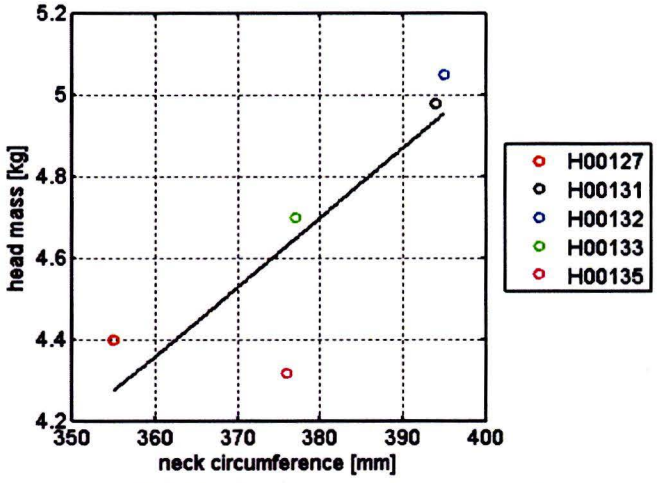

Figure 3.4 Relation head mass and neck circumference

As stated in section 3.3.2, the neck circumference is used by Irwin to scale the geometry of the neck in every direction. It does not seem implausible to scale the geometry of the neck in x- and y-direction with the neck circumference. However, there is doubt about using the neck circumference to calculate the scale factor for the z-direction. To investigate this relation, the neck lengths of the five volunteers are plotted as function of their neck circumference in Figure 3.5.

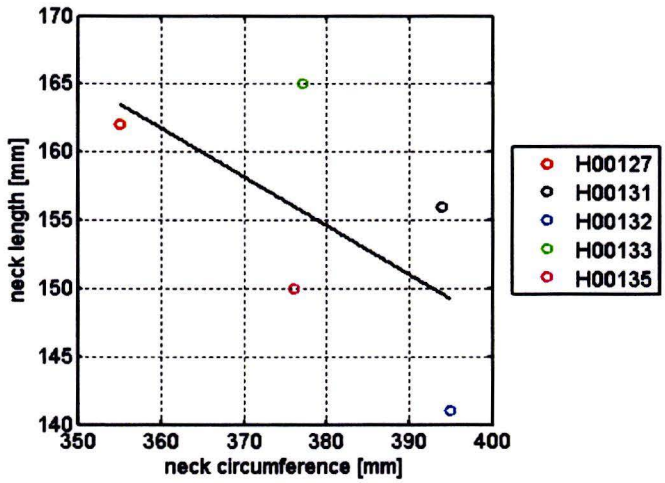

Figure 3.5 Relation neck length and neck circumference

As can be seen in this figure the regression model does not describe the data accurately, this is confirmed by the value for R^2, presented in Table 3.8. The value for ρ indicates that a negative relation is likely.

There are also cases in which the erect sitting height (*ESH*) is used to scale the length of the neck (Mertz et al., 1984 and 1989). The *ESH* of the NBDL human subjects is plotted as function of their neck length to investigate the correlation, as shown in Figure 3.6. The R^2 assesses that the regression model is not accurate but the value of ρ indicates a possible positive relation between both parameters, see Table 3.8.

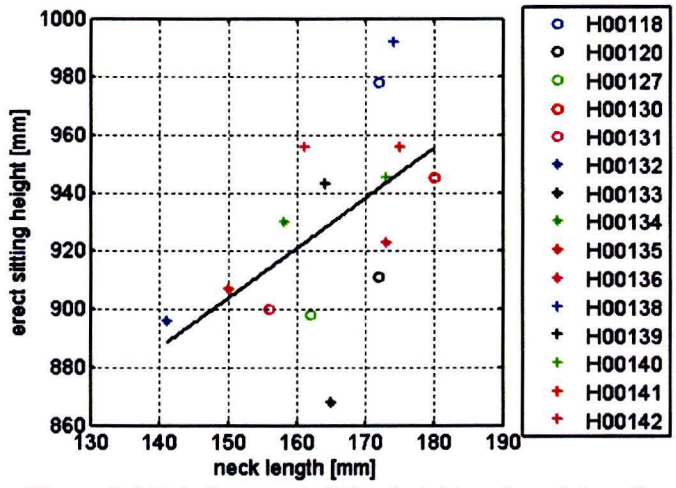

Figure 3.6 Relation erect sitting height and neck length

3.4.5 Conclusions from the NBDL volunteer analysis

From the volunteer analysis some relations were found:

- It was found that there is no relation between both the flexion and the twist of the head and the neck length of the volunteers, as is displayed in Figure 3.2a and Figure 3.2b, respectively. Except for some extreme values the data points were all between 50 and 55 degrees, so they were almost the same. Only a small variation in the head flexion was observed between the subjects. The statistical values were low, which also indicates that a linear relation is not realistic.

- A linear relation was found between the neck length and the maximum head displacements in lateral and vertical direction for this set of human subjects, as shown in Figure 3.2c and Figure 3.2d.

- With respect to the head mass, no relation to the kinematic head responses was observed, as can be seen in Figure 3.3a and Figure 3.3d. This could be explained by the expectation that a heavier head is carried by a stronger neck. The plot of the head mass as a function of the neck circumference was an indication that this is the case, as can be seen in Figure 3.4. It should nevertheless be stated here that an increase in neck strength does not necessarily mean that the neck muscle size increases too (Conley et al., 1997). However, as already stated in section 3.2.2, the maximum force that neck muscles can apply does not play a significant role in unexpected, severe impacts since there is not sufficient time for the volunteer to reach this state.

- It is likely that the relation between neck circumference and neck length is negative, as shown in Figure 3.5. Therefore, if the neck length is assumed to scale with the neck circumference, it would become shorter as the neck circumference increases. Nevertheless, it should be kept in mind that this relationship is based on data of only five volunteers and the values of ρ and R^2 are only -0.61 and 0.36, respectively. Therefore this relation may not be realistic.

- The relation between the neck length and the erect sitting height is likely to be positive, as can be seen in Figure 3.6. However, also this relation was not very strong as presented in Table 3.8.

3.5 NBDL volunteer analysis vs. scaling method of Irwin

The analysis of the male NBDL volunteers showed some relations between the anthropometry of the head-neck system and the peak responses of the head in lateral direction, see section 3.4.5. The question that now arises, is whether these relations also apply to male/female differences. Ono et al. (2007) found that the kinematic head responses to unexpected (no muscle tension) shoulder impact of female subjects was similar to the response of the male subjects. Both male and female volunteers had approximately 50th percentile anthropometry, as can be seen in Table 3.9. The available anthropometric measurements of volunteers in several studies are compared to the anthropometry of the standard 50th percentile male and female.

Table 3.9 Anthropometry of subjects in several studies compared to the standard size

Anthropometry	Standard 50th		Vasavada (2001)		Harty (2004)		Ono (2007)	
	*female	**male	female	male	female	male	female	male
standing height [mm]	1626	1751	1640	1770			1630	1754
erect sitting height [mm]	859	907					857	936
neck circumference [mm]		383	360	390	342	400		
neck length [mm]					123.5	124.5		
head circumference [mm]		574	560	580	557	592		
head mass [kg]		4.54					3.8	4.4
weight [kg]	62.5	78.2	65	77			51.7	70.6

* Tilley (1993)
** Schneider (1983)

The neck length of midsize males and females is similar (see section 3.2.1). Furthermore, the factor between the sitting height of a 1st female and a 50th female is similar to the ratio between a 1st male and a 50th male, 0.89 and 0.90 respectively (Tilley, 1993). These conclusions indicate that the relations found for males can also be applied to females. Table 2.7 shows that Irwin's requirements for vertical peak head displacement for females exceed those for males. This also applies to head flexion and head twist. As small females have shorter necks than average males, their peak head displacements should be smaller than for the midsize male. The flexion and twist angles do not have to be scaled since male and female head-neck systems have a similar range of motion in lateral bending as was found in several studies, as stated in section 3.2.1.

So again a major contradiction between this study and the head-neck scaling method of Irwin was found, which indicates the need for new head response requirements for small females in the lateral NBDL setup. Therefore, new scaling rules as well as new peak response requirements will be developed in the following section.

3.6 New scaling rules and response requirements

From the literature study and the analysis of the NBDL volunteer tests the following was found.

In the lateral NBDL tests, the input to the head-neck system, the T1 response, is similar for all volunteers. Irwin proposes a method to scale the response of T1 for small females, but during this present study, no extensive research has been done to verify this method. Although it seems reasonable to scale the response of T1 based on differences in shoulder geometry between males and females, similar T1 responses have been found for female and male volunteers in the tests conducted by Ono et al. (2007). It has also been found that the T1 responses were highly dependent on the interaction between the restraint systems and the thorax (Wismans and Spenny, 1983). To eliminate these influencing factors in the test, the head-neck system of the dummy could be separated from the rest of the model. If the rotations of T1 are found small enough to be neglected, lateral translation is the only relevant T1 motion. In this case, the average T1 acceleration measured on the midsize male volunteers as well as the T1 acceleration measured on the 50^{th} WS in the lateral NBDL tests could be used as input to the head-neck system. This test setup was already proposed by Wismans and Spenny (1983).

Since the neck length is not available in the anthropometry database of Schneider et al. (1983) and no convincing relation was found between the neck length and the erect sitting height, it is chosen to stick with the assumption that the neck length scales with the neck circumference, although this relation is not confirmed in this study.

From the literature study it was found that the cantilever beam representation only applies for volunteers who have their neck tensed at maximum force prior to impact. The muscle activation of the NBDL volunteers was not measured, however they were asked to relax prior to and during the impact. It might be the case that some muscle activation occurred during the test, but definitely not to maximum force level. Therefore, for the new scaling rules no difference between neck stiffness is assumed between 5^{th} female and 50^{th} male.

No major shortcomings were found to invalidate the assumption of Irwin to model the whole head-neck system as a spring-mass system, although some minor drawbacks are present. The assumption that the head is considered as a point mass in the head CG and the rotation about OC is not fully accounted for, are indeed shortcomings of the model. However, response scaling should be as accurate as possible and yet relatively simple. The current head-mass model meets this requirement. Therefore, corresponding equations based on this model do not need to be modified.

Below the new scaling rules are summarized:

1) Separate testing of head-neck system; no scaling of T1 response
2) The neck stiffness is not scaled, so the peak head displacement relative to T1 in lateral and vertical direction scales with the neck length
3) Also, both the head flexion and the head twist do not have to be scaled
4) For the timing and accelerations the equations of Irwin are still valid

The peak head displacements are scaled with the neck length scale factor as illustrated in Figure 3.7.

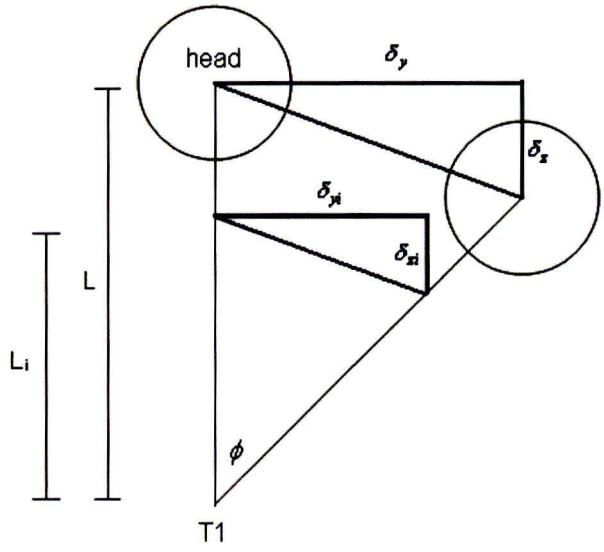

Figure 3.7 Scaling peak head CG displacements with neck length

Here, L and L_i are the neck lengths of the standard and the target subject, respectively. Assuming the angle ϕ to be invariant to the neck length and the neck length to decrease, the triangle decreases with the same factor as the neck length.

The new response requirements for the head displacements can now be calculated as follows:

$$\delta_{yi} = \delta_y \lambda_{z\,neck} \qquad 3\text{-}1$$

$$\delta_{zi} = \delta_z \lambda_{z\,neck} \qquad 3\text{-}2$$

The head twist and flexion angles do not need to be scaled, and the scaling factors for the timing of maximum excursion, R_{th}, the lateral head CG acceleration, R_{ahy}, as well as the vertical head CG acceleration, R_{ahz}, are given as (see also 2-23 to 2-25):

$$R_{th} = \sqrt{\frac{\lambda_{m\,head}}{\lambda_{k\,Mx}}}, \qquad 3\text{-}3$$

$$R_{ahy} = \lambda_v \sqrt{\frac{\lambda_{k\,Mx}}{\lambda_{m\,head}}}, \qquad 3\text{-}4$$

$$R_{ahz} = \frac{(\lambda_v)^2}{\lambda_{z\,neck}}, \qquad 3\text{-}5$$

where λ_{kMx} is equal to one, since neck bending stiffness does not need to be scaled.

The new head-neck response requirements for a small female head-neck system in lateral NBDL setup are presented in Table 3.10, together with the original requirements for the midsize male and the small female.

Table 3.10 New 5th female response requirements for the head-neck segment test based on the lateral NBDL test

		Requirements 50th Male		Requirements 5th Female (Irwin)		New Requirements 5th Female	
Response		Lower	Upper	Lower	Upper	**Lower**	**Upper**
Peak horizontal acc T1	*g*	12	18	15	22	**12**	**18**
Peak hor. displ. T1 wrt sled	mm	46	63	38	51	**46**	**63**
Peak hor. displ. head CG wrt T1	mm	130	162	121	151	**103**	**128**
Peak vert. displ. head CG wrt T1	mm	64	94	80	118	**51**	**75**
Time of max head excursion	s	0.159	0.175	0.161	0.177	**0.143**	**0.158**
Peak lateral acc head CG	*g*	8	11	8	11	**9**	**12**
Peak vertical acc head CG	*g*	8	10	10	13	**10**	**13**
Peak flexion angle	deg	44	59	56	75	**44**	**59**
Peak twist angle	deg	45	32	57	41	**45**	**32**

4. Evaluation of the 5th female WS head-neck design

4.1 Methodology

The second objective of this study was to evaluate the head-neck system of the 5th WS according to valid peak response requirements, in this case the newly developed requirements described in section 3.6. In the recent lateral, full-scale NBDL test with the 5th WS prototype, the T1 responses did not meet the requirements for acceleration and displacement, as was described in section 2.3.5. Since this response of T1 is the input to the head-neck system, the head responses, measured during the hardware test, cannot be compared directly to the new response requirements. Therefore, the evaluation was carried out by means of simulations in MADYMO using only the head-neck system with measured T1 accelerations as input (Wismans and Spenny, 1983), see section 3.6. MADYMO (MAthematical DYnamic MOdel) is a multi-body software code, which is widely used in the field of impact safety to study the dynamic behavior of systems of rigid bodies connected by kinematic joints. To evaluate the responses of the 5th WS head-neck system by means of simulations, the test setup, displayed in Figure 4.1, was used.

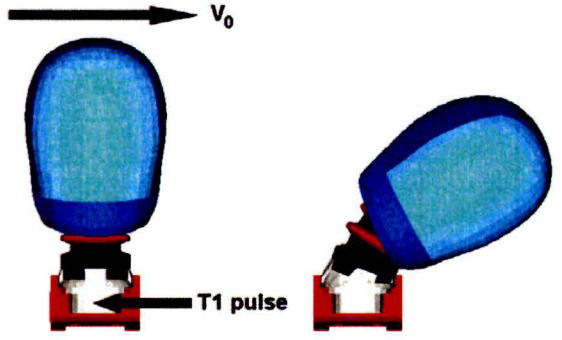

Figure 4.1 Numerical head-neck model of 50th WS at t=0 (left) and at t=max excursion (right). V_0 is the sled velocity.

To investigate how the numerical head-neck system of the 5th WS prototype corresponds with its hardware counterpart, the head responses of the numerical model of the 5th WS were compared with those of the 5th WS prototype. Here, the lateral T1 acceleration and, if necessary, rotation, measured on the 5th WS prototype was used as input.

Next, the numerical head-neck model of the 5th WS was evaluated using the newly developed response requirements. A T1 acceleration measured on hardware 50th WS (Been et al., 2004 was used as input, since it meets the requirements for the T1 peak response. This also holds for the average of the T1 accelerations measured on the NBDL male volunteers. In addition, the newly developed requirements were checked by investigating whether the differences between the responses of the numerical 50th and the 5th WS model were consistent with the differences between the original NBDL and the newly developed 5th female peak response corridors.

To perform these simulations, a numerical model of the 5th WS head-neck had to be created, since no good model of the 5th WS was available. A new numerical model of the 5th WS was developed by scaling down a numerical model of the 50th WS, which was developed in MADYMO. All body regions of this numerical 50th WS model were validated for side impact (MADYMO Model Manual). To validate the numerical head-neck model of the 50th WS for the lateral NBDL tests, the test setup proposed in section 3.6 is used. The T1 acceleration measured on the 50th WS was used as input to its numerical head-neck system. The simulation setup, shown in Figure 4.1, was used.

Finally, the biofidelity rating method, described in section 2.2.4, was used to quantify the biofidelity of the head-neck system with respect to the new response requirements. Although the accuracy of the biofidelity rating method is limited, since it only takes into account peak values, it is widely accepted in biomechanics and often used throughout the APROSYS project. Because of the limitation of the biofidelity rating method, also the trends in the responses were evaluated.

4.2 Numerical model of the 50th male WorldSID

4.2.1 Simulation setup

The head-neck model of the 50th WS was taken from the MADYMO numerical quality dummy model (Q-dummy) of the 50th WS.

The geometry is based on technical drawings and 3D laser scans of the actual hardware dummy. Masses, centers of gravity and moments of inertia were calculated on the basis of component mass measurements and 3D CAD drawings (MADYMO Model Manual). The contact surface of the head is modeled by facet surfaces representing the head skin and face. For visualisation purposes, internal surfaces like the head core are included as well.

The neck column is modeled with six bodies. The upper and lower bodies represent the top and bottom plates, the four bodies in between together represent the rubber neck mould, respectively. The OC is located just above the top plate and T1 just below the bottom plate as can be seen in Figure 4.2. In this figure, the numerical head-neck model of the 50th WS is presented as it is modeled from the hardware head and neck, shown in Figure 2.6. The neck bracket is modeled as well. The geometry of the neck consists of facet surfaces.

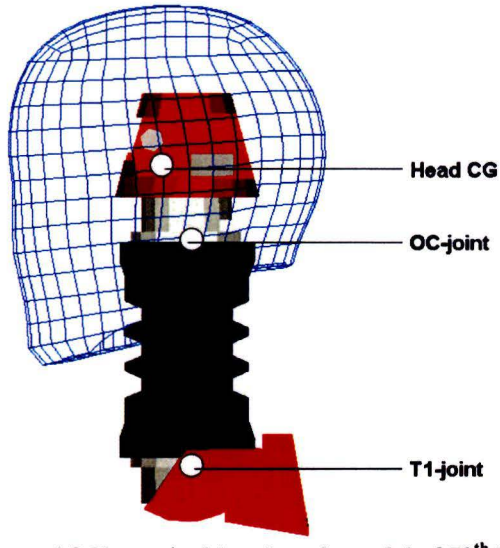

Figure 4.2 Numerical head-neck model of 50th WS

The bodies of the head-neck system are connected by joints. Spherical joints connect the neck top plate to the head and the neck bottom plate to the neck bracket. Restraints on these joints represent the compliance of the deforming neck buffers. The compliance of the rubber neck mould is represented by restraints on free joints in between the neck mould bodies.

A number of component tests have been carried out for development and validation of the numerical 50th WS model. All tests for which the head-neck system is validated are listed in Table 4.1.

Table 4.1 Validation tests for head and neck of the numerical 50th WS model

Component	Test description	Test specification	
Head	Lateral drop test	Drop height / angle	150 mm / 35 deg
			200 mm / 35 deg
			200 mm / 10 deg
Neck	Pendulum swing tests	Velocity	2.5 m/s^2
			3.4 m/s^2
			4.0 m/s^2

As can be seen in Table 4.1 the 50th WS numerical model has not yet been validated for the lateral NBDL test. This has been done during this study using the methodology described earlier.

The measured lateral T1 acceleration from the experimental tests with the 50th WS in the lateral NBDL setup (Been et al., 2004) was prescribed to T1 in the simulation with the numerical head-neck model.

However, during the experimental tests of the 50th WS in the lateral NBDL test setup, not only lateral motion but also T1 rotations were observed. The maximum lateral flexion angle was 2 degrees and the peak head twist angle of T1 was 4 degrees. The T1 rotations are shown in Figure 4.3 and Figure 4.4.

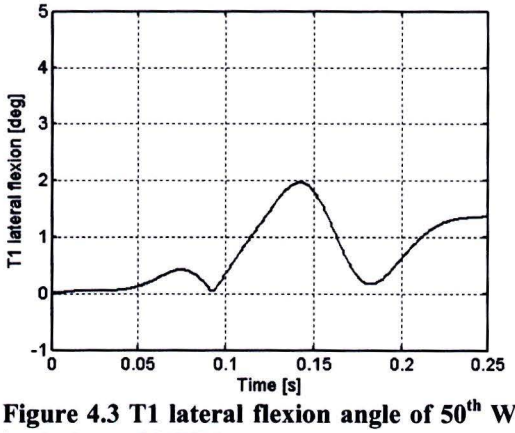

Figure 4.3 T1 lateral flexion angle of 50th WS in the lateral NBDL test

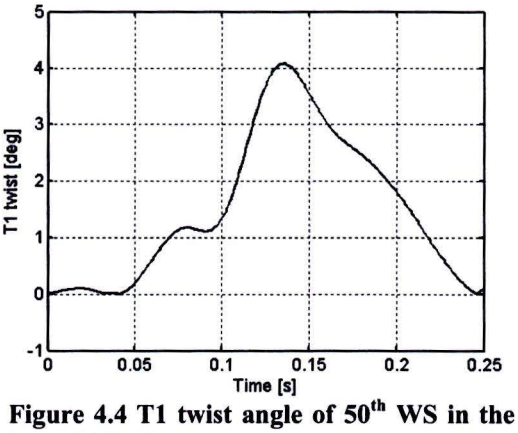

Figure 4.4 T1 twist angle of 50th WS in the lateral NBDL test

Although it was expected that these rotations would only have a minor, or even a negligible effect on the head responses, this was checked through simulations. To be able to prescribe the T1 rotations, an extra joint had to be added to the numerical head-neck model as it is not possible to prescribe accelerations as well as rotations to one single joint.

4.2.2 Simulation results and discussion

Figure 4.5 to Figure 4.10 show the head responses of the simulation with the numerical head-neck model of the 50th WS (blue) compared to the measured head responses in the full-scale lateral NBDL test with the hardware 50th WS (black). The response requirements for the 50th WS are inserted in red.

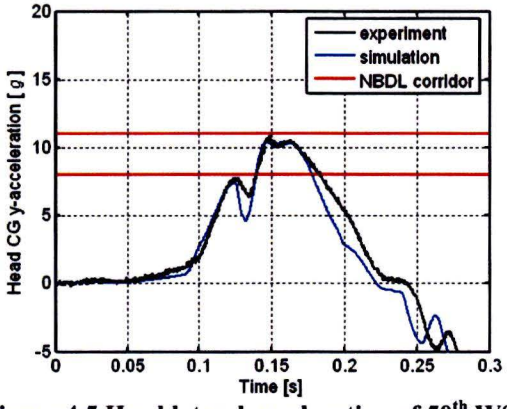

Figure 4.5 Head lateral acceleration of 50th WS

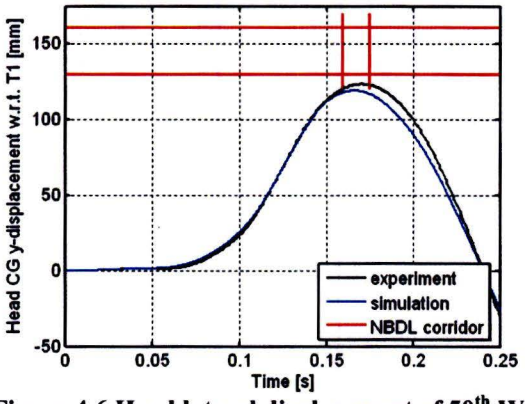

Figure 4.6 Head lateral displacement of 50th WS

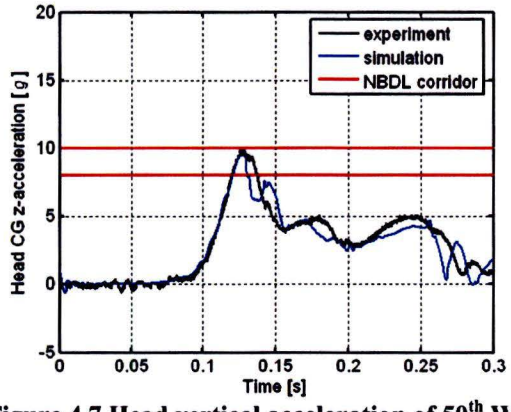

Figure 4.7 Head vertical acceleration of 50th WS

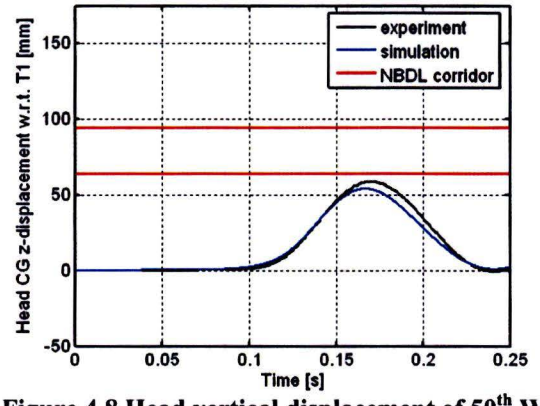

Figure 4.8 Head vertical displacement of 50th WS

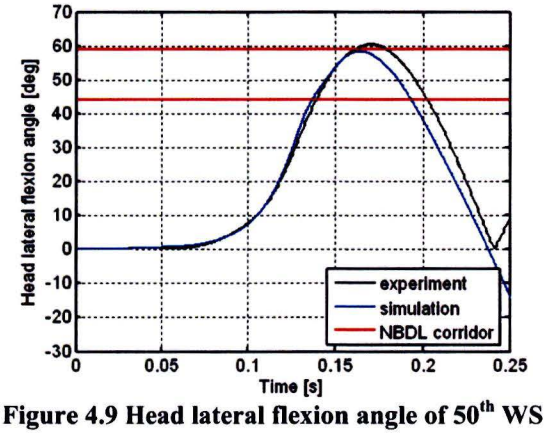

Figure 4.9 Head lateral flexion angle of 50th WS

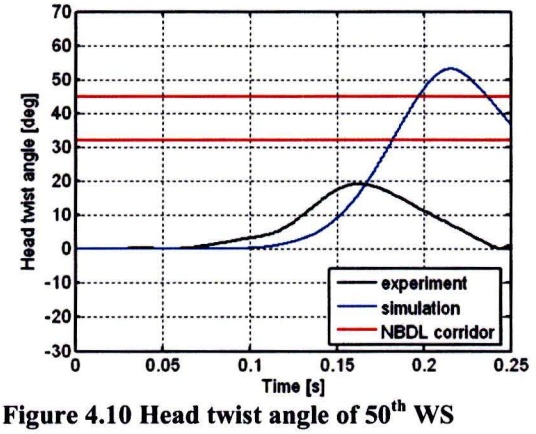

Figure 4.10 Head twist angle of 50th WS

In Table 4.2 the peak responses measured on the 50th WS in the lateral NBDL test and the corresponding peak responses of the numerical head-neck model are presented. In addition, also the ISO biofidelity rating is calculated and included.

Table 4.2 Peak responses of hardware and numerical 50th WS in NBDL setup

Responses 50th WS		NBDL Requirements		Experiment	Simulation
		Lower	Upper		
Peak horizontal acc T1	*g*	12	18	12.7	12.7
Peak hor. displ. T1 wrt sled	mm	46	63	46.1	46.1
Peak hor. displ. head CG wrt T1	mm	130	162	123.6	119.1
Peak vert. displ. head CG wrt T1	mm	64	94	58.7	53.7
Time of max head excursion	s	0.159	0.175	0.170	0.167
Peak lateral acc head CG	*g*	8	11	10.9	10.4
Peak vertical acc head CG	*g*	8	10	9.8	9.8
Peak flexion angle	deg	44	59	60	58
Peak twist angle	deg	45	32	20	53
Biofidelity rating				7.5	8.2

As can be seen in Figure 4.5 and Figure 4.7 the head peak accelerations are equal. The peak head displacements in both the simulation as well as the experiment are situated just below the peak response corridors. However, the peaks of the displacements in the simulations are slightly lower. This also holds for the head flexion angle. The peak head flexion angle in the simulation is situated in the peak response corridors whereas the one in the experiments is just outside. Except for the head twist it is found that the responses in the simulation match the responses in the experiment well.

The difference in head twist between the simulation and the experiment is large: 34 degrees. In the experiments the twist was too low with respect to the response requirements, since new buffers in the neck of the hardware 50th WS add torsional stiffness (Been et al., 2004). The numerical model does not account for that extra torsional stiffness in the neck and therefore shows a head twist that is larger than the response requirements. Since the weight factor of the twist is the smallest (so least important) of all responses in the biofidelity rating, as presented in Table 2.4, this mismatch is not further investigated in this study.

The biofidelity rating for the hardware 50th WS is 7.5 and for the numerical one 8.2, so both models have 'good' head-neck biofidelity. The difference in rating can mainly be dedicated to the mismatch between the peak of the lateral head flexion angle and the corresponding requirement. The peak in the simulations just meets the requirements whereas the peak in the experiment just does not.

Figure 4.11 and Figure 4.12 show two of the lateral responses of the head, once in simulations with a rotating T1 (magenta) and once with a non-rotating T1 coordinate system (blue). The head responses in the experimental test (black) as well as the corresponding peak response corridors (red) are shown as well. Other responses are presented in Figure C.1 to Figure C.6 in appendix C.

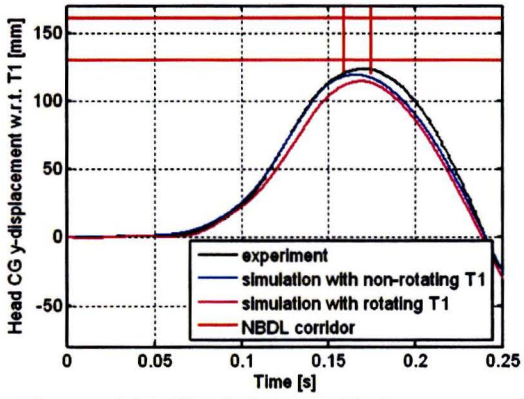

Figure 4.11 Head lateral displacement of the 50th WS w.r.t. a non-rotating and a rotating T1 coordinate system

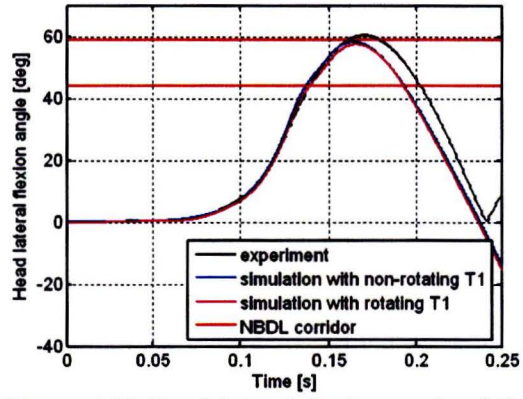

Figure 4.12 Head lateral flexion angle of the 50th WS w.r.t. a non-rotating and a rotating T1 coordinate system

These simulations show that the influence of the rotation of T1 on the head responses is present, but indeed negligible.

Summarising, it can be stated that the numerical head-neck model of the 50th male WS represents its hardware counterpart well except for its head twist. In addition, this resemblance also shows that it is sufficient to only prescribe the lateral T1 acceleration to the head-neck model to check its biofidelity. Taken into account that this numerical head-neck model has also been validated for a pendulum swing test at 3 different velocities, as given in Table 4.1, it can be stated that the model is robust.

4.3 Numerical model of the 5th female WorldSID

4.3.1 Simulation setup

The anthropometry database of Schneider et al. (1983) and scale factors derived by Irwin (2002) were used to define the geometry and mass properties of the 5th WS prototype, as described in (Barnes et al., 2005). This method was also used to develop a numerical head-neck model of the 5th WS from the numerical head-neck model of the 50th WS. Segment masses, centers of gravity, relative distances between bodies and joints were scaled with the factors defined for head and neck. Inertia properties were derived by using the scaling method presented by Morsink et al. (2000), since no clear method for scaling inertia is described by Irwin. The masses of accelerometers were not scaled, since they are the same for the 50th and 5th WS.

Since the geometry of the neck mould was scaled as well, the restraints on the free joints in between the bodies of the neck mould have to be modified. These restraint functions are given in N/m. To account for the geometry change of the mould, the restraint functions were scaled with the scale factor for the neck length.

After scaling the numerical head-neck model of the 50th WS, a comparison between the 5th WS prototype, as described in Martinez et al. (2006) and the numerical 5th WS head-neck model showed the following:

- The total mass of the 5th WS numerical head-neck model as well as its separate segment masses are almost similar to those of the hardware prototype. The mass of the numerical head-neck system was 0.25 kg (6%) larger than that of the prototype. This difference was found to be located in the neck.

- The distance between the defined locations of the OC and T1 is 92 mm in the numerical model, whereas it is stated in the report of Martinez et al. (2006) that this distance is 95 mm in the hardware 5th WS.

It was assumed that these minor differences between the numerical and hardware dummy are too small to result in major differences in the head responses.

Two simulations with the numerical head-neck model of the 5th WS have been carried out with each a different input for the T1 acceleration as described in section 4.1. The T1 acceleration measured on the 5th WS prototype is shown in Figure 2.17. The average T1 acceleration of the NBDL male volunteers and the T1 acceleration of the hardware 50th WS are displayed in Figure 4.13 and Figure 4.14, respectively.

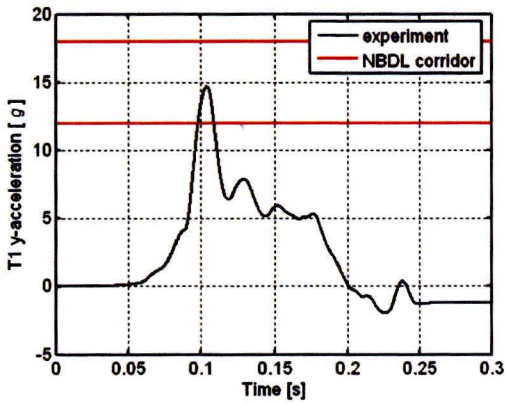

Figure 4.13 Average NBDL volunteer T1 acceleration (ISO TR 9790)

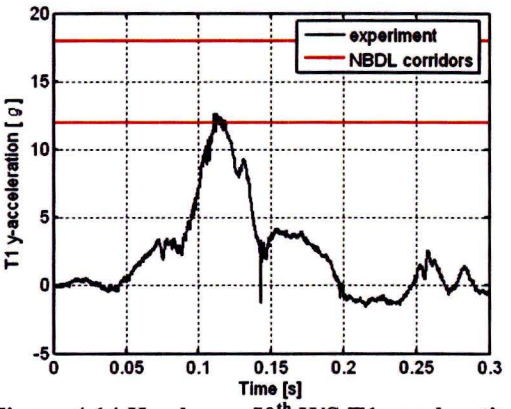

Figure 4.14 Hardware 50th WS T1 acceleration (Been et al., 2004)

In the full-scale sled tests with the 5th WS prototype in the lateral NBDL setup, small rotations of T1 were measured. The peak lateral flexion and peak twist of T1 were 2.2 and 5.9 degrees, respectively. The flexion of T1 in time is shown in Figure 4.15 and the twist in Figure 4.16. Both angles are in the same order as the measured T1 rotations on the 50th WS, nevertheless the trend is different. Therefore, in addition, a simulation was conducted to check the influence of these rotations. The results of these simulations are presented in appendix C.

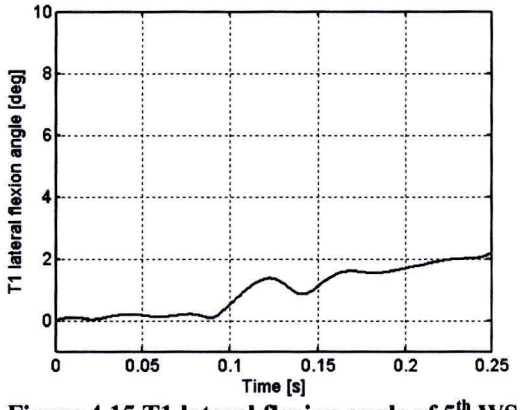

Figure 4.15 T1 lateral flexion angle of 5th WS prototype in the lateral NBDL test

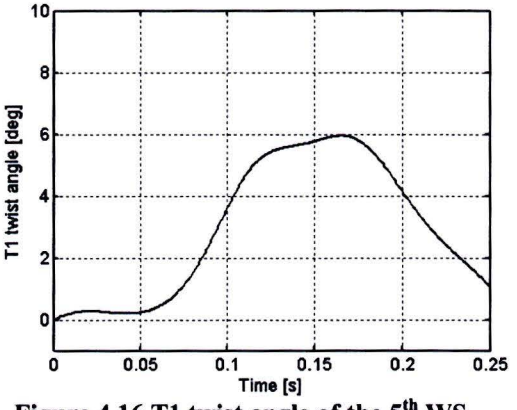

Figure 4.16 T1 twist angle of the 5th WS prototype in the lateral NBDL test

4.3.2 Simulation results and discussion

Figure 4.17 to Figure 4.22 show the head responses of the numerical 5th WS head-neck model compared to the head responses of the 5th WS prototype in the sled test. The peak values of all responses can be found in Table 4.3.

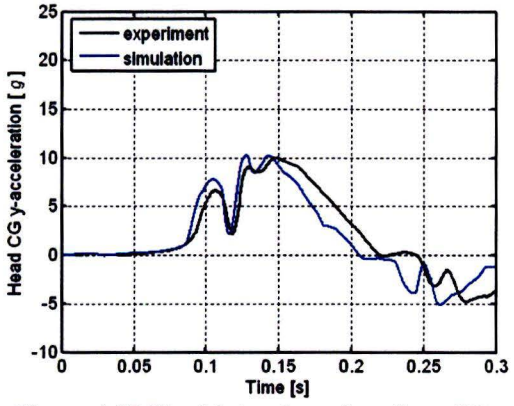

Figure 4.17 Head lateral acceleration of the 5th WS

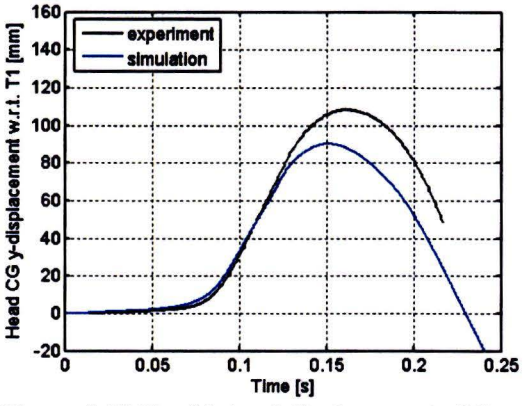

Figure 4.18 Head lateral displacement of the 5th WS

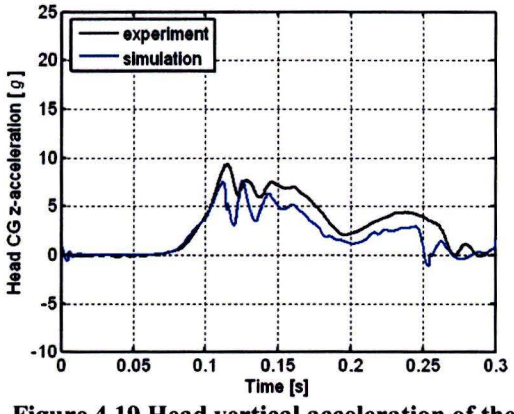

Figure 4.19 Head vertical acceleration of the 5th WS

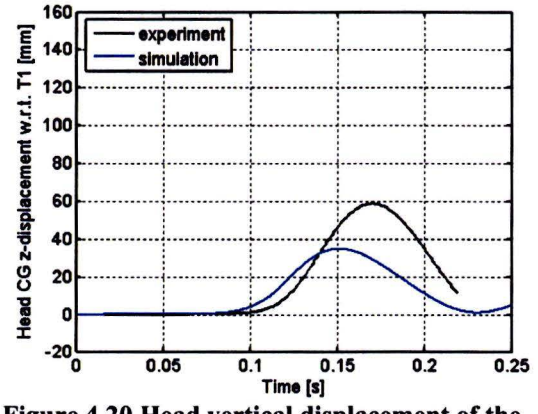

Figure 4.20 Head vertical displacement of the 5th WS

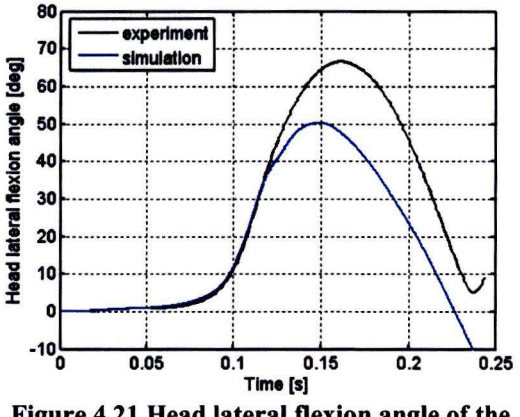

Figure 4.21 Head lateral flexion angle of the 5th WS

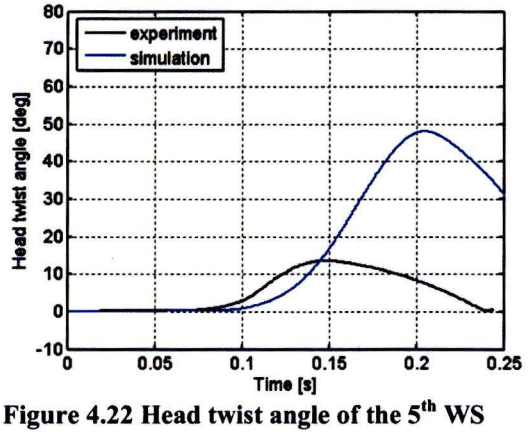

Figure 4.22 Head twist angle of the 5th WS

Table 4.3 Peak responses of the numerical 5th WS and 5th WS prototype

Responses 5th WS		Experiment	Simulation
Peak horizontal acc T1	*g*	10.0	10.0
Peak hor. displ. T1 wrt sled	mm	28.1	28.1
Peak hor. displ. head CG wrt T1	mm	108.2	90.0
Peak vert. displ. head CG wrt T1	mm	56.0	34.9
Time of max head excursion	s	0.158	0.151
Peak lateral acc head CG	*g*	10.1	10.3
Peak vertical acc head CG	*g*	9.4	7.7
Peak flexion angle	deg	66	50
Peak twist angle	deg	13	48

Figure 4.17 shows that the head lateral acceleration of the numerical model was similar to the one measured in the experiment. The trend of both lines in Figure 4.17 is approximately the same, only the overshoot at 0.11 seconds is a little higher in the simulation. After the peak the head lateral acceleration in the simulation is lower than in the experiment. This could be caused by a difference in inertia, for in the simulations the head moves faster in time than in the experiment.

However, the lateral and vertical displacement, the vertical acceleration as well as the flexion angle of the head, shown in Figure 4.18 to Figure 4.21, were all too small in comparison to the responses measured during the sled test. Nevertheless, the trend of the responses until the peak is similar. The peaks are reached earlier in the simulations than in the experiment. These observations implicate that 5th WS prototype has smaller neck stiffness than the numerical neck. This could be the case since the neck design of the prototype is based on the assumption of Irwin that the stiffness of a female neck is less than that of a male (Barnes et al., 2005).

The head twist angle, again, was found much larger in the simulation than in the experiment. This was also observed for the head twist of the numerical model of the 50th WS. Again, this effect can be explained by the buffers that were implemented in the hardware neck which was not accounted for in the numerical model, see also 4.2.2.

In test laboratories the design of a prototype is often changed a little to make it work properly in a calibration test. These changes are often not well registered and thus not accounted for in the numerical model. Therefore, this can also be a cause of differences between the simulation- and test results.

The influence of rotations of T1 on the head-neck responses was found to be small. The head accelerations with respect to a non-rotating T1 coordinate system were similar to those with respect to a rotating T1. The kinematic head responses were somewhat smaller with respect to a rotating T1. The largest discrepancy between a rotating and non-rotating T1 is observed in the peak of the lateral displacement of the head (5%). All other head responses show much smaller differences. Figure C.7 to Figure C.12 in appendix C show this simulation.

The head responses of simulations with both the numerical head-neck model of the 50th WS and that of the 5th WS are shown in Figure 4.23 to Figure 4.28. The response requirements for the peak head responses of the 50th WS (in blue) as well as of the 5th WS (in red) are shown too. Note that the response requirements for the head angles are equal for both models. In addition, the upper boundary of the peak head vertical acceleration for the 50th WS is equal to the lower boundary for the 50th WS, as can be seen in Figure 4.25. Figure 4.13 shows the T1 acceleration that was used as input for the simulations.

The ratio between the peak response of the 5th WS and that of the 50th WS is calculated and compared to the theoretical ratio, which is equal to the response scale factor as defined in section 3.6. As long as the difference between both ratios is smaller than or equal to 0.05, the ratios from theory are considered to be similar to ratios observed in the simulation results.

The peak values of the responses, the corresponding response ratios as well as the theoretical ratios are presented in Table 4.4. Also, the biofidelity rating is presented in this table.

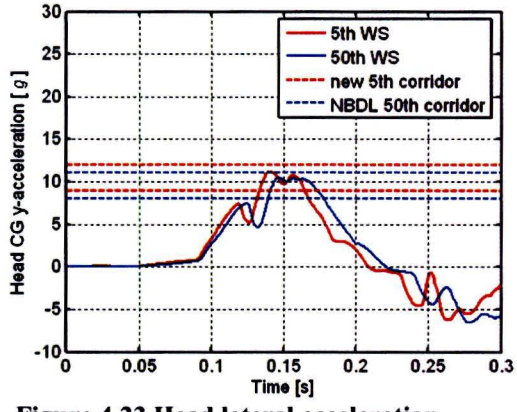

Figure 4.23 Head lateral acceleration (input: 50th WS T1 acceleration)

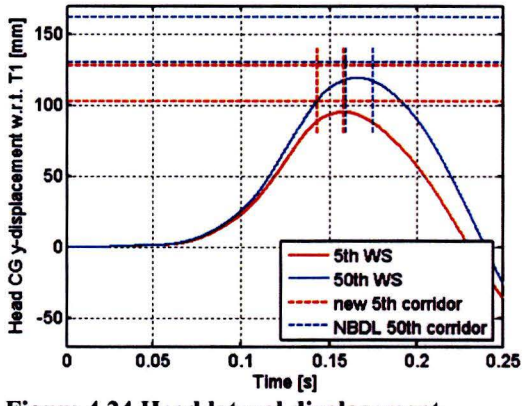

Figure 4.24 Head lateral displacement (input: 50th WS T1 acceleration)

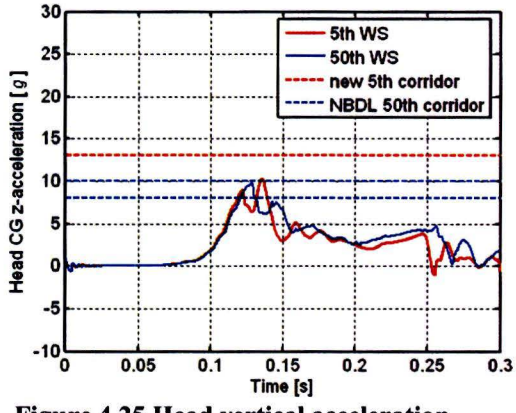

Figure 4.25 Head vertical acceleration (input: 50th WS T1 acceleration)

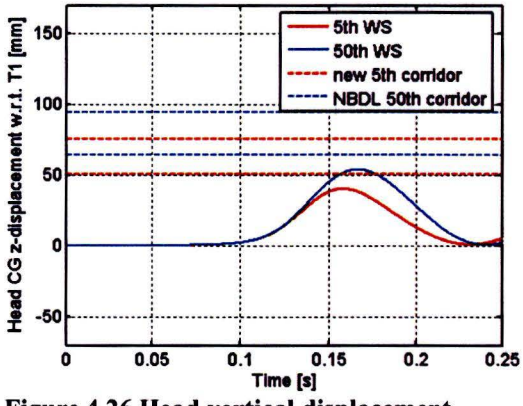

Figure 4.26 Head vertical displacement (input: 50th WS T1 acceleration)

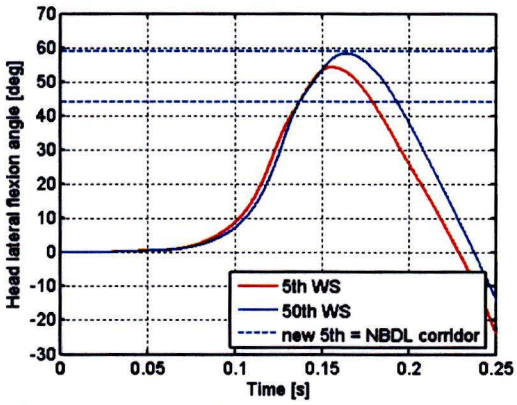

Figure 4.27 Head lateral flexion angle (input: 50th WS T1 acceleration)

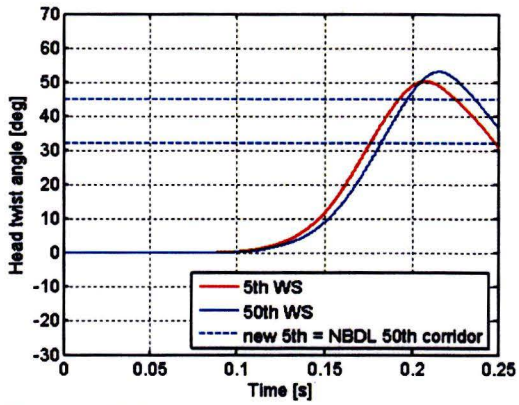

Figure 4.28 Head twist angle (input: 50th WS T1 acceleration)

Table 4.4 Head responses of numerical 50th WS compared to those of the numerical 5th WS (input: 50th WS T1 acceleration)

Responses		numerical 50th WS	numerical 5th WS	num ratio 5th vs 50th WS	theory ratio 5th vs 50th WS
Peak horizontal acc T1	*g*	12.7	12.7	1.00	1.00
Peak hor. displ. T1 wrt sled	mm	46.1	46.1	1.00	1.00
Peak hor. displ. head CG wrt T1	mm	119.1	95.2	0.80	0.79
Peak vert. displ. head CG wrt T1	mm	53.7	40.2	0.75	0.79
Time of max head excursion	s	0.167	0.158	0.95	0.90
Peak lateral acc head CG	*g*	10.4	11.1	1.07	1.10
Peak vertical acc head CG	*g*	9.8	10.4	1.06	1.30
Peak flexion angle	deg	58	54	0.93	1.00
Peak twist angle	deg	53	51	0.96	1.00
Biofidelity rating	-	8.2	8.2		

The peak head accelerations in lateral, shown in Figure 4.23, and vertical direction, shown in Figure 4.25, were situated just inside the peak response corridor for the 5th WS as well as for the 50th WS. However, the ratio between the peaks of the 50th and the 5th WS in the simulations was smaller than the corresponding ratio defined according to the scaling analysis, especially for the acceleration in vertical direction. This can be explained by the fact that the acceleration vector, shown in Figure A.9, does not point exactly to T1 during the whole time period to maximum head excursion. Therefore, the acceleration ratio between 50th and 5th WS is larger in theory than in the simulation.

For the lateral peak head displacement of the 50th and 5th WS numerical model, shown in Figure 4.24, it can be stated that the ratio between the responses in the simulation was similar to that of the requirements in section 3.6. The ratio for the vertical head displacements of the simulations, displayed in Figure 4.26, is slightly smaller than the theoretical one.

The lateral flexion angle of the 5th WS model is slightly smaller than that of the 50th WS, as presented in Figure 4.27. This difference is not exactly the same as the one predicted in scaling analysis but well within 0.05. This also holds for the head twist angle of the numerical 5th WS compared to that of the 50th WS model, as can be seen in Figure 4.28.

It was observed that the responses of the numerical head-neck model of the 5th WS meet the newly developed requirements well, as can be seen in the figures. The biofidelity rating of the numerical 5th WS is similar to that of the numerical 50th WS. Both values classify the numerical head-neck model as 'good', just like the head-neck system of the hardware 50th WS.

In addition, the responses of the numerical head-neck model of the 50th WS as well as that of the 5th WS were have been evaluated and compared using the average T1 acceleration of the NBDL volunteers as input. These responses are presented in Figure C.13 to Figure C.18 in appendix C. Table 4.5 shows the peak responses of the numerical 50th and 5th WS as well as the ratios between the peak responses of both models. The biofidelity rating is presented too.

Table 4.5 Head responses of numerical 50th WS compared to those of the numerical 5th WS (input: average T1 acceleration of NBDL volunteers)

Responses		numerical 50th WS	numerical 5th WS	num ratio 5th vs 50th WS	theory ratio 5th vs 50th WS
Peak horizontal acc T1	*g*	14.7	14.7	1.00	1.00
Peak hor. displ. T1 wrt sled	mm	54.2	54.2	1.00	1.00
Peak hor. displ. head CG wrt T1	mm	122.7	97.6	0.80	0.79
Peak vert. displ. head CG wrt T1	mm	57.8	43.6	0.75	0.79
Time of max head excursion	s	0.170	0.161	0.95	0.90
Peak lateral acc head CG	*g*	10.8	12.0	1.11	1.10
Peak vertical acc head CG	*g*	11.9	12.8	1.08	1.30
Peak flexion angle	deg	60	56	0.93	1.00
Peak twist angle	deg	55	52	0.95	1.00
Biofidelity rating	-	7.0	7.7		

The results of this evaluation are similar to those presented in Table 4.4. Since the peak of the lateral head flexion angle of the numerical 5th WS head-neck model is situated inside the peak response corridor and that of the 50th WS model is just not, its biofidelity rating is 0.7 lower than that of the numerical model of the 5th WS. Otherwise, it would have been the same. Both values classify the neck model as 'good'.

The influence of a scaled T1 acceleration for the 5th WS on its head responses was investigated by prescribing the T1 acceleration of the hardware 50th WS scaled according to the T1 response scaling method of Irwin, as is shown in Figure C.19 in appendix C. The responses are shown in Figure C.20 to Figure C.25. It was observed that the major difference in the responses is that the timing of the peaks is earlier and the peaks are shifted slightly upwards.

4.3.3 Conclusions

From the comparison of the head responses between the simulation and the experiment with the 5th WS, displayed in Figure 4.17 to Figure 4.22, can be concluded that there are some discrepancies between the numerical model and the prototype. Therefore, it is stated that the numerical 5th WS head-neck model does not correspond to the head-neck system of the 5th WS prototype as it is tested recently. A clear statement about the design of the current 5th WS prototype cannot be made, based on this comparison. According to the results of the other simulations with the numerical head-neck model of the 5th WS, it could be recommended to increase the neck bending stiffness of the 5th WS prototype and to lower the neck torsional stiffness.

According to these simulations it was found that the numerical 5th WS, scaled according to the geometry scaling method of Irwin except for scaling of the neck stiffness, meets the newly developed peak response requirements well. Furthermore, the numerical head-neck model of the 5th WS has good biofidelity, just like that of the numerical 50th WS and that of the hardware 50th WS.

The ratio found between the responses of the numerical 5th WS and those of the numerical 50th WS is similar to the difference between the response requirements of NBDL for the midsize male and the newly developed response requirements for the small female.

5. Conclusions and recommendations

Full-scale sled tests in the lateral NBDL setup have been conducted with the 5th WS prototype. Not all head-neck responses met the corresponding peak response requirements proposed by Irwin et al. (2002). To investigate this discrepancy, two major objectives were formulated for the present study:

1. Analysis of the head-neck scaling method proposed by Irwin et al. (2002), for both geometry as well as response.

2. Evaluation of the head-neck design of the 5th WS according to valid peak response requirements.

For the analysis of the scaling method an extensive literature review was carried out and the peak head responses of the midsize male volunteers in the original lateral NBDL tests were analysed. For the evaluation of the head-neck design simulations in MADYMO were performed with a numerical model of the 5th WS. The most important conclusions from this research are presented in the following.

- The assumption of Irwin et al. to use the same scale factor to scale both the neck length as well as the neck circumference is not confirmed in this study. Therefore, its validity is still uncertain.

- New response scaling rules and requirements for head-neck system were developed in this study. Herein, the neck stiffness is not scaled, as was found in literature. The response scaling method of Irwin et al. (2002) does account for a maximum difference in neck stiffness, since it has been found that males can exert higher forces with their neck muscles than females can (Schneider et al., 1975; Vasavada et al., 2002). However, if no pretension of the neck muscles is present, the time it takes to reach this maximum force is greater than the time to maximum head excursion (Schneider et al., 1975). So the difference in possible neck stiffness does not have to be accounted for in scaling the head-neck responses in unexpected, lateral impact (Ono et al., 2007) like for instance, the lateral NBDL tests (Ewing et al., 1977). In addition, it can be concluded that the head-neck response scaling method of Irwin et al. (2002) is not suitable to scale the response requirements of midsize males to corresponding requirements for a small female.

- Simulations with a numerical head-neck model of the 5th WS show that its head responses meet the newly developed requirements. This 5th WS numerical model was scaled down from the well-validated numerical head-neck model of the 50th WS according to the geometry scaling method of Irwin et al. (2002). It was also found that the rotations measured on T1 in the hardware experiments have a negligible effect on the head responses.

- The difference between the head responses of the 50th WS numerical model and those of the 5th WS numerical model is comparable to the difference between the NBDL and newly developed response requirements. This resemblance confirms the consistency of the new requirements and shows that these are more biofidelic for unexpected side impact than the original response requirements of Irwin et al. (2002).

Based on this study the following recommendations can be made:

- When developing new crash test dummies starting from the size of a 50th percentile male by scaling to other dimensions, it would be better to separate the neck scale factor in anatomical *z*-direction from the scale factor in *x*- and *y*-direction instead of using the same factor for all directions. This factor can be based on measured neck length, for example the distance between the first and last cervical vertebra, or, in absence of this measurement, on the erect sitting height (Mertz et al., 1989).

- For an update of the 5th female WS, it is advised to use equal neck stiffness properties as were used for the 50th WS. The numerical head-neck system of the 5th WS has been developed with the geometry scaling rules of Irwin et al. (2002) and meets the newly developed peak response requirements. Therefore, it is most likely that if the head-neck geometry of the 5th WS prototype could be developed similarly, its peak head responses would meet the newly developed requirements as well.

- For next validation tests of the 5th WS prototype, it is recommended to check the peak head and neck responses with respect to the new requirements, developed in this study. Since there is doubt about scaling the T1 response it is recommended to conduct a sled test with only the head-neck system of the 5th WS using a T1 acceleration of the 50th WS as input.

- Finally, for more exact research on differences in the head-neck anthropometry as well as responses between midsize males and small females it is recommended to conduct volunteer tests. This could also lead to more insight in the differences between the shoulder response of males and females.

References

Anscombe F.J. (1973). Graphs in statistical analysis. *American Statistician*, Vol. 27, pp. 17-21.

Barnes A., Been B. (2005). *APROSYS WorldSID 5th Female Requirements*. Deliverable Report 5.2.1.

Been B., Philippens M., Lange R. de, Ratingen M. van (2004). WorldSID Dummy Head-Neck Biofidelity Response. *Stapp Car Crash Journal*, Vol. 48, paper No. 2004-22-0019, pp. 431-454.

Choi H., Vanderby R. (1999). Comparison of biomechanical human neck models: Muscle forces and spinal loads at C4–C5 level. *Journal of Applied Biomechanics,* Vol 15, pp. 120-138.

Cohen, J. (1988). *Statistical power analysis for the behavioral sciences* (2nd edition) Hillsdale, NJ: Lawrence Erlbaum Associates.

Conley M.S., Stone M.S., Nimmons M. (1997). Specificity of resistance training responses in neck muscle size and strength. *European Journal of Applied Physiology*; Vol. 75, pp. 443–448.

Dalley F. (1998). *Interactive atlas of human anatomy*. Novartis.

Ewing C. L., Thomas D.J., Lustik L., Muzzy III W.H., Willems G.C. and Majewski P. L.(1977), Dynamic response of the human head and neck to +Gy Impact Acceleration. *Proceedings of the 21st Stapp Car Crash Conference*, pp. 549-586.

Ewing C. L., Thomas D.J., Lustik L., Muzzy III W.H., Willems G.C. and Majewski P. L.(1978), Effect of initial position on the human head and neck response to +y Impact Acceleration. *Proceedings of the 22nd Stapp Car Crash Conference*, pp. 103-138.

Fenner R.T. (1989). *Mechanics of solids*. Oxford, Blackwell Scientific Publications.

Harty J.A., Quinlan J.F., Kennedy J.G., Walsh M., O'Byrne J.M. (2004). Anthropometrical analysis of cervical spine injuries. *Injury*, Vol. 35, pp. 249-252.

Irwin A.L., Mertz H.J., Ali M. Elhagediab A.M., Moss S. (2002), Guidelines for Assessing the Biofidelity of Side Impact Dummies of Various Sizes and Ages, *Stapp Car Crash Journal*, Vol. 46, paper No. 2002-22-0016, pp. 297-319.

ISO Technical Report 9790 (1999). *Road vehicles –anthropometric side impact dummy-Lateral response requirements to assess the biofidelity of the dummy.* ISO/TC22/SC12/WG5 Document N455 – Final edition.

ISO TG N393 (1999). *User's manual for the WorldSID 50th percentile male side impact dummy*. TC22/SC12/WG5 WorldSID.

ISO TG N399 (1999). *WorldSID Mechanical Requirements and Drawing Lists.* TC22/SC12/WG5 WorldSID.

Martínez L., Ferichola G., Garcia A.; Guerra L.J. (2006) *APROSYS: INSIA WorldSID 5th percentile female dummy anthropometry study*, APROSYS SP 5.2.

McConville J.T., Churchill T.D., Kaleps I., Clauser C.E., Cuzzi J. (1980). *Anthropometric relationships of body and body segment moments of inertia.* Report AFAMRL-TR-80-119. Airforce Aerospace Medical Research Lab. Wright Patterson Airforce Base, Ohio.

Meijer R., Philippens M. (2007). *Biofidelity testing of the 5th female WorldSID head-neck response*. Aprosys SP 5.2, Deliverable D5.2.5.

Mertz H.J. (1984). A Procedure for Normalizing Impact Response Data. *SAE transactions*, Vol. 93, 4, pp. 4.351-4.358, paper No. 840884.

Mertz H.J., Irwin A.L., Melvin J.W., Stalnaker R.C., and Beebe M.S. (1989). *Size, Weight and Biomechanical Impact Response Requirements for Adult Size Small Female and Large Male Dummies*. Society of Automotive Engineers, Warrendale, PA, USA.

Mertz H.J., Prasad P., Irwin A.L. (1997). Injury Risk Curves for Children and Adults in Frontal and Rear Collisions. *Proceedings of the 41st Stapp Car Crash Conference*. pp. 13-30.

Montgomery, D.C., Runger, G.C. (1999). *Applied statistics and probability for engineers*, second edition. New York: Wiley.

Mordaka J.K., (2004). *Finite element analysis of whiplash injury for women.* PhD thesis. Nottingham Trent University.

Moroney SP, Schultz AB, Miller JAA. (1988). Analysis and measurement of neck loads. *Journal of Orthopaedic Research,* Vol. 6, *5,* pp. 713-720.

Morsink P.L.J., Happee R., Brugman F.J., Lange R. de (2000). *MADYSCALE A scaling procedure of occupant models withtin MADYMO.* TNO report: 00.OR.BV.005.1/PM.

Ono K., Ejima S., Kaneoka K., Fukushima K., Yamada S., Ujihashi S. (2007) Biomechanical Response of Head/ Neck/ Torso and Cervical Vertebral Motion to Lateral Impact Loading on the Shoulders of Volunteers. *Proceedings of 21st International Technical Conference on the Enhanced Safety of Vehicles*, paper No. 07-0294.

Patrick, L.M., Chou, C.C., 1976. *Response of the Human Neck in Flexion,Extension and Lateral Flexion.* VRI-7.3. Society of Automotive Engineers, Warrendale, PA, USA.

People Size (1998). *Computer Anthropometric Database.* Open Ergonomics Ltd. Leicestershire, UK.

Samaha R.R. and Elliot D.S. (2003) .NHTSA Side Impact Research: Motivation for Upgraded Test Procedures. *Proceedings of 18th International Technical Conference on the Enhanced Safety of Vehicles*, paper No. 492.

Scheider L.W., Foust D.R., Bowman B.M., Snyder R.G., Chaffin D.B., Baum J.K. (1975), Biomechanical properties of the human neck in lateral flexion, *Proceedings of the 19th Stapp Car Crash Conference*, paper No. 751155, pp. 455-486.

Schneider L.W., Robbins D.H., Pflug M.A., and Snyder R.G. (1983). *Development of Anthropometrically Based Design Specifications of an Advanced Adult Anthropomorphic Dummy Family. Vol. 1.* NHTSA Contract No. DTNH22-80-C-07502.

Tarriere C. (1986). *Proposal for Lateral Neck Response Requirements for Severe Impact Conditions*, ISO/TC22/SC12/WG5 Document N166-Draft 1.

Thunnissen J., Wismans J., Ewing C.L. and Thomas D.J. (1995). Human volunteer head-neck response in frontal flexion: A new analysis. *Proceedings of the 39th Stapp Car Crash Cornference*, paper No. 952721, pp. 439-460.

Tilley A.R. (1993) *The measure of man and woman*, revised edition. New York: John Wiley & Sons

TNO MADYMO BV. (2005). *MADYMO Model Manual.* Version 6.3.

USA Department of Defence (1980). *Military handbook anthropometry of U.S. military personnel.*

Vasavada A.N., Li S. and Delp S.L. (2001), Three-dimensional isometric strength of neck muscles in humans. *Spine*, Vol. 26, 17, pp. 1904-1909.

Wismans J., Spenny C. H. (1983). Performance requirements for mechanical necks in lateral flexion. *Proceedings of the 27th Stapp Car Crash Conference*, paper No. 831613, pp 137-148.

Wismans J., Van Oorschot H. and Woltring J. H. (1986). Omni-directional head-neck response. *Proceedings of the 30th Stapp Car Crash Conference*, paper No. 861893, pp. 313-331.

Youdas J.W., Garrett T.R., Suman V.J., Bogard C.L., Hallman H.O., Carey J.R. (1992). Normal Range of Motion of the Cervical Spine: An Initial Goniometric Study. *Physical Therapy*, Vol. 72, 11, pp. 770-780

www.neurosurgeon.org/pem/pdf/20040418_SpineAnatomyandSpineGeneral.pdf Congress of Neurological Surgeons (05-09-2007)

www.worldsid.org (05-09-2007)

A. Head-neck scaling method of Irwin

Irwin et al. (2002) developed guidelines for assessing the biofidelity of side impact dummies. The anthropometry database of Schneider (1983) is used in this study to define scale factors for different parameters. The anthropometry of the small female and midsize male is shown in Table 2.6.

Table A.1 Standard size anthropometry (Schneider et al., 1983)

Description	Units	Small Female	Mid Male
Standing height	mm	1513	1751
Erect sitting height	mm	812	907
Head circumference	mm	534	574
Head width	mm	145	154
Head depth	mm	183	197
Neck circumference	mm	304	383
Head mass	kg	3.67	4.54
Neck mass	kg	0.77	1.54
Total body mass	kg	46.72	78.20

These anthropometry data are an average of measurements taken from volunteers as presented in the following section.

A.1 Anthropometry measurements

The anthropometry measurements of Table 2.6 are taken as explained by the following figures (Military handbook of anthropometry U.S. military personnel, 1980) and descriptions:

85 Head width (Figure A.1) - The maximum breath of the head, usually above and behind the ears.

86 Head circumference (Figure A.1) – the maximum horizontal circumference of the head.

90 Head depth, or height (Figure A.2) – the maximum length of the head, from forehead to back of head.

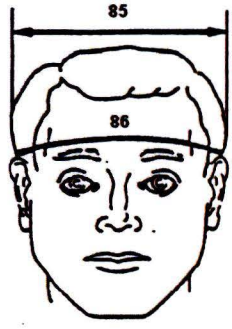

Figure A.1 head with and circumference

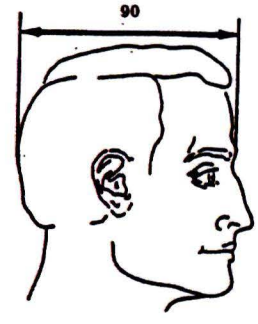

Figure A.2 Head depth

133 Neck circumference (Figure A.3) – the circumference of the neck at Adam's apple level.

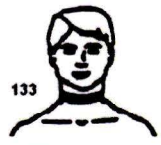

Figure A.3 Neck circumference

157 Erect sitting height (Figure A.4) – the vertical distance from sitting surface to top of the head.

163 Stature or standing height (Figure A.5) – vertical distance from the floor to the top of the head.

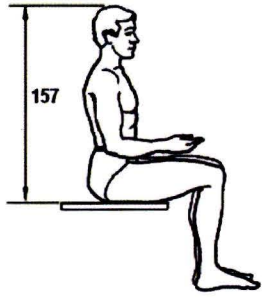

Figure A.4 Erect sitting height

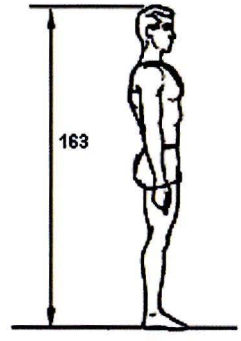

Figure A.5 Stature

A.2 Head-neck scaling of geometry and properties

From the anthropometry database of the USA adult population (Schneider et al., 1983) the key body segments lengths and weights, on which the scale factors are based, are selected. These factors are defined to assure that the mass density of each body segment is the same as for the corresponding segment of the Hybrid III. In every database the body segment weights are estimated from the length measurements and a particular way of dividing the body in different sections, a sectioning scheme. The mass of the segments for the two new sized dummies had to be calculated again, for the body sectioning scheme of Schneider et al. (1983) is not the same as the one used for the Hybrid III dummy. These constraints of equal density and unknown weights lead to the assumption that the head geometry is considered to be a sphere and is scaled by a characteristic length factor:

$$\lambda_{x\,head} = \lambda_{y\,head} = \lambda_{z\,head} = \frac{(C+W+D)_i}{(C+W+D)_{mid\,male}}, \qquad \text{A-1}$$

where C is the head circumference, W the head width and D the head depth.

The following equation forms the basis for the derivation of the head mass scale factor:

$$\rho = \frac{m}{V}, \qquad \text{A-2}$$

Where ρ is the density, m the mass and V represents the volume. The head is assumed to be a sphere and the volume of a sphere is:

$$V_{sphere} = \frac{4}{3}\pi r^3, \qquad \text{A-3}$$

where r is the radius of the sphere. For geometrically similar objects with equal density, the mass scale ratio λ_m can be calculated by taking the cube of the characteristic length. For the head this leads to:

$$\lambda_{m\,head} = (\lambda_{x\,head})^3. \qquad \text{A-4}$$

The density scale factor is given by λ_ρ and is calculated as follows:

$$\lambda_\rho = \frac{\rho_i}{\rho_{mid\,male}}. \qquad \text{A-5}$$

The density scale factor is set to one, because there is no difference between the mass density of a small female and that of a mid size male.
The moment of inertia of a solid sphere is the basis for derivation of the scale factor of the head moment of inertia:

$$I = \frac{2mr^2}{5}. \qquad \text{A-6}$$

The mass of the sphere is given by m and r is the radius. The scale factor for the moment of inertia of the head is written as:

$$\lambda_{Iz\,head} = \lambda_{m\,head}(\lambda_{x\,head})^2. \qquad \text{A-7}$$

The geometrical scale factor of the neck is based on the neck circumference (NC). This scale factor is used in every direction:

$$\lambda_{x\,neck} = \lambda_{y\,neck} = \lambda_{z\,neck} = \frac{(NC)_i}{(NC)_{midmale}}. \qquad \text{A-8}$$

The mass scale factor of the neck ($\lambda_{m\ neck}$) is based on a cylinder with height h and radius r for which the volume is calculated as:

$$V_{cilinder} = \pi r^2 h, \qquad \text{A-9}$$

$$\lambda_{m\,neck} = (\lambda_{x\,neck})^3 \lambda_\rho, \qquad \text{A-10}$$

where λ_ρ is equal to 1. The elastic modulus of either bone or soft tissue is scaled as follows:

$$\lambda_{E\,j} = \frac{E_{j_i}}{E_{j\,midmale}}. \qquad \text{A-11}$$

E is the elastic modulus and j represents bone or soft tissue. Because there is no difference between the elastic modulus of either bone or soft tissue of different sized adults, the scale factor is one.

With respect to lateral sled tests it is useful to calculate two stiffness ratios for the neck: the bending stiffness and the neck twist stiffness. To calculate the bending stiffness of the neck, it is assumed to behave like a cantilever beam, as shown in. The angle ϕ and displacement u of the free end of a cantilever are calculated as follows (Fenner, 1989):

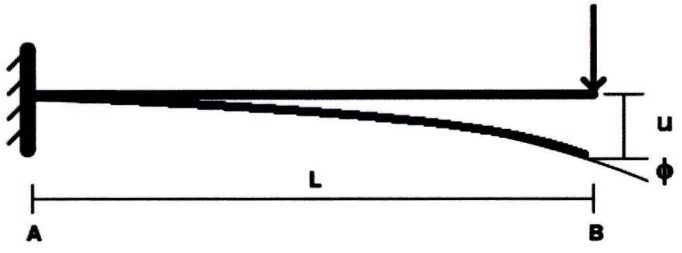

Figure A.6 Cantilever beam (Fenner, 1989)

$$\phi = \frac{FL^2}{2EI}, \qquad \text{A-12}$$

$$u = \frac{FL^3}{3EI}, \qquad \text{A-13}$$

where F is the applied force, L is the length of the beam, E is the elastic modulus of the material of which the beam is made, and I area moment of inertia.

The bending stiffness is:

$$k_{bending} = \frac{F}{u} = \frac{3EI}{L^3}, \qquad \text{A-14}$$

with, for a cylindrical cross section of the beam:

$$I_{circle} = \frac{\pi r^4}{4}, \qquad \text{A-15}$$

where r is again the radius of the cylinder. Combining equations A-14 and A-15 leads to the equation for bending stiffness of a cantilever beam:

$$k_{bending} = E\frac{3\pi r^4}{4L^3}. \qquad \text{A-16}$$

From this, the scale factor of the neck bending stiffness is derived:

$$\lambda_{k\,Mx\,neck} = \lambda_{E\,soft}\frac{(\lambda_{y\,neck})^4}{(\lambda_{z\,neck})^3} = \lambda_{E\,soft}\lambda_{y\,neck}. \qquad \text{A-17}$$

Note here that λ_{Esoft} is one and therefore can be omitted. The equation for torque T of a cylindrical shaped beam around it length axis (Fenner, 1989) is the basis to derive the torque of the neck around its z-axis:

$$T = \frac{GJ\theta}{L} = \frac{T}{\theta} = k_{twist} = \frac{GJ}{L}. \qquad \text{A-18}$$

G is the shear modulus of the neck, θ is the twist angle and J is the polar second moment of inertia of the neck, which is assumed to be a cylinder with radius r:

$$J_z = \frac{\pi r^4}{2}. \qquad \text{A-19}$$

Combining these equations leads to an equation for the twist stiffness:

$$k_{twist} = G\frac{\pi r^4}{2L}. \qquad \text{A-20}$$

From A-20 the neck twist scaling factor can be derived:

$$\lambda_{k\,Mz\,neck} = \lambda_{G\,neck}\frac{(\lambda_{y\,neck})^4}{\lambda_{z\,neck}} = \lambda_{G\,neck}(\lambda_{y\,neck})^3, \qquad \text{A-21}$$

where λ_{Gneck} is the scale factor of the shear modulus, which is equal to the shear modulus:

$$\lambda_{G\,neck} = \frac{G_{neck\,i}}{G_{neck\,midmale}}. \qquad \text{A-22}$$

It is calculated in the same way as the density and is set to one since the shear modulus of the neck is based on the elasticity of the soft tissue.

A.3 Head-neck response scaling

To calculate the lateral neck bending angle, the head neck system is modeled as a spring with a point mass on it. The spring represents the neck and has the properties of the cantilever beam. The point mass models the head mass. The spring is attached to the point mass at the head CG as can be seen in Figure 2.15.

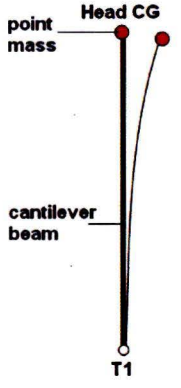

Figure A.7
Mass-spring representation of the head-neck system

The kinetic energy of the system is converted to elastic energy of the spring:

$$\frac{1}{2}mv^2 = \frac{1}{2}ku^2 \rightarrow u = v\sqrt{\frac{m}{k}}. \qquad \text{A-23}$$

Here, v is the velocity of the head, m is the head mass and k the neck bending stiffness. The relation between the deflection and angle can be derived from A-12 and A-13:

$$u = \frac{2L}{3}\phi. \qquad \text{A-24}$$

Combining equation A-23 and A-24 results in an equation for the lateral bending:

$$\phi = \frac{3v}{2L}\sqrt{\frac{m}{k}}. \qquad \text{A-25}$$

This can be converted into a scaling equation to calculate the lateral bending scaling factor. The response scaling factors are denoted by R:

$$R_{\phi} = \frac{\lambda_v}{\lambda_{z\,neck}} \sqrt{\frac{\lambda_{m\,head}}{\lambda_{k\,Mx}}}, \qquad \text{A-26}$$

λ_v is the velocity scale factor. It is calculated in the standard way (see equation 2-2) and also set to 1, since no difference is present. To derive the scale factor for the twist angle the same method as for the bending angle can be used, though adjusted to the direction:

$$\frac{1}{2} I_{head} \omega^2 = \frac{1}{2} k_{twist} \theta^2 \rightarrow \theta = \omega \sqrt{\frac{I_{head}}{k_{twist}}}, \qquad \text{A-27}$$

where ω is the angular velocity:

$$\omega = \frac{v}{r_{head}}. \qquad \text{A-28}$$

These equations together give the twist angle of the head:

$$\theta = \frac{v}{r_{head}} \sqrt{\frac{I_{head}}{k_{twist}}}. \qquad \text{A-29}$$

From this the twist angle scale factor can be derived:

$$R_{\theta} = \frac{\lambda_v}{\lambda_{x\,head}} \sqrt{\frac{\lambda_{Iz}}{\lambda_{k\,Mz}}}. \qquad \text{A-30}$$

The approach for deriving the lateral and vertical head displacement is described now. In Figure A.8 $u_{mid\ male}$ is the peak head displacement of the mid size male and it is derived as:

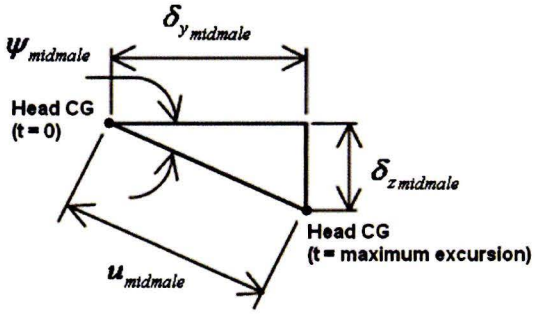

Figure A.8 Dimensions used to calculate peak head displacements (Irwin et al., 2002)

$$u = \sqrt{\delta_y^2 + \delta_z^2}\ . \qquad \text{A-31}$$

The scale factor for this displacement R_u is (see equation A-24):

$$R_u = \lambda_v \sqrt{\frac{\lambda_{m\,head}}{\lambda_{k\,Mx}}}\ . \qquad \text{A-32}$$

The angle $\psi_{midmale}$ is scaled by equation A-26 (R_ϕ). To calculate the peak displacements δ of the head, first the angle ψ_i and scaled displacement u_i need to be calculated. Using these, the peak displacements of the head in lateral δ_{yi} and vertical direction δ_{zi} are calculated:

$$\psi_i = R_\phi \psi_{midmale}, \qquad \text{A-33}$$

$$u_i = R_u u_{midmale}, \qquad \text{A-34}$$

$$\delta_{yi} = u_i \cos(\psi_i), \qquad \text{A-35}$$

$$\delta_{zi} = u_i \sin(\psi_i). \qquad \text{A-36}$$

The maximum head excursion period scale factor is calculated from the simple equation:

$$t = \frac{u}{v}, \qquad \text{A-37}$$

where t is time. If this equation A-37 is combined with A-23, the time period scale factor can be calculated:

$$R_{th} = \sqrt{\frac{\lambda_{m\,head}}{\lambda_{k\,Mx}}}\ . \qquad \text{A-38}$$

The acceleration ratio in lateral direction R_{ahy} is based on the standard relations of a mass spring model (Mertz et al., 1984 and 1989) that is discussed above:

$$R_{ahy} = \lambda_v \sqrt{\frac{\lambda_{k\,Mx}}{\lambda_{m\,head}}}\ . \qquad \text{A-39}$$

The vertical non-impact acceleration scale factor of the head (R_{ahz}) is calculated from the acceleration in circular motion:

$$a = \frac{v^2}{R}, \qquad \text{A-40}$$

where a is the centrifugal acceleration and here r represents the radius of the circle. Converted to the system of the head and neck, the scale factor is calculated as:

$$R_{ahz} = \frac{(\lambda_v)^2}{\lambda_{z\,neck}}. \qquad \text{A-41}$$

Figure A.9 shows the accelerations of the head in the mass-spring model of the head-neck system.

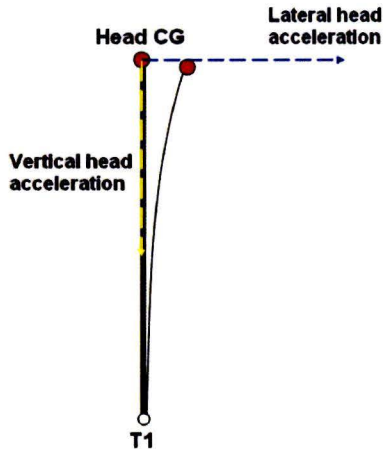

Figure A.9 Head accelerations in mass-spring representation of the head-neck system

B. Statistics

Regression analysis is a statistical technique for modeling and investigating the relationship between two or more variables (Montgomery and Runger, 1999). Using these statistics it is possible to find estimates for the parameters of a regression equation, or regression model, which estimates the values of y as function of variable x. Normally, the first step to be taken is to make a scatter plot of all data, with the one variable on the x-axis and the other on the y-axis. If those data points are almost in a straight line, simple linear regression can be used. Then y would be:

$$y = \beta_0 + \beta_1 x + \varepsilon, \qquad \text{B-1}$$

where β_0 and β_1 are the unknown regression coefficients for respectively the intercept and the slope and ε is a random error of the model. Also higher order regression models can be chosen, for example second order:

$$y = \beta_0 + \beta_1 x + \beta_2 x^2 + \varepsilon, \qquad \text{B-2}$$

with an extra regression coefficient β_2. The least squares method can be used to define the estimates for β_0 and β_1 for n pairs of observations $(x_i,y_i...x_n,y_n)$. With this method the sum of the squares of the vertical deviations is minimized, as displayed in Figure B.1.

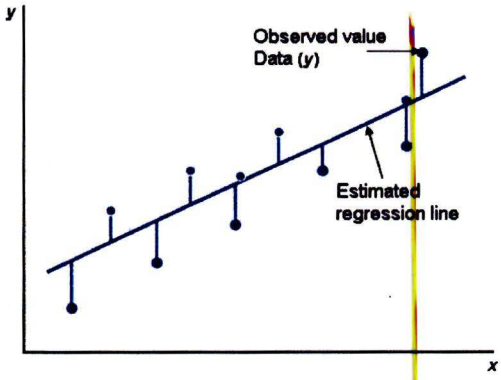

Figure B.1 Deviations of the data from the estimated regression model (Montgomery and Runger, 1999)

The least squares estimate $\hat{\beta}_0$ and $\hat{\beta}_1$ of respectively β_0 and β_1 in a simple linear regression model are:

$$\hat{\beta}_0 = \bar{y} - \hat{\beta}_1 \bar{x}, \qquad \text{B-3}$$

$$\hat{\beta}_1 = \frac{\sum_{i=1}^{n} y_i x_i - \frac{\left(\sum_{i=1}^{n} y_i\right)\left(\sum_{i=1}^{n} x_i\right)}{n}}{\sum_{i=1}^{n} x_i^2 - \frac{\left(\sum_{i=1}^{n} x_i\right)^2}{n}}, \qquad \text{B-4}$$

$$\bar{y} = \frac{1}{n}\sum_{i=1}^{n} y_i, \qquad \text{B-5}$$

$$\bar{x} = \frac{1}{n}\sum_{i=1}^{n} x_i, \qquad \text{B-6}$$

To assess the adequacy of the regression model the coefficient of determination R^2 is used. It defines the amount of variability in the data explained by or accounted for by the regression model. R^2 ranges between zero and one. A value of one means that the model accounts for all variability and zero means the opposite. The value for R^2 is calculated as:

$$R^2 = \frac{SS_R}{SS_T}, \qquad \text{B-7}$$

$$SS_R = \sum_{i=1}^{n}\left(\hat{y}_i - \bar{y}\right)^2, \qquad \text{B-8}$$

$$SS_E = \sum_{i=1}^{n}\left(y_i - \hat{y}_i\right)^2, \qquad \text{B-9}$$

$$SS_T = SS_R + SS_E, \qquad \text{B-10}$$

where $\hat{y}_i$ is the estimated value of y. The coefficient of determination is actually the square of the correlation coefficient ρ. This is a parameter to check the linearity between two random variables. It is defined as:

$$\rho = \frac{\mathrm{cov}(x,y)}{\sqrt{V(x)V(y)}}, \qquad \text{B-11}$$

where cov(x,y) is the covariance between variable x and variable y and $V(x)$ is the variance in x. The values for ρ can vary between minus one and one. A negative value close to one means there is a negative linear relation, a value of zero means there is no

relation and a value of one means there is a positive linear relation. In Table B.1 some values for ρ are presented which represent small, medium or large correlation.

Table B.1 Quality of correlation and corresponding values for ρ (Cohen, 1988)

Correlation	Positive values of ρ
Small	0.01 to 0.29
Medium	0.30 to 0.49
Large	0.50 to 1.00

If ρ is smaller than 0.10 no relation is considered to be present. The value of the correlation coefficient alone is not necessarily sufficient to evaluate the presence of a linear relation between variables. Figure B.2 shows four different scatter plots with the same value for ρ (Anscombe, 1973).

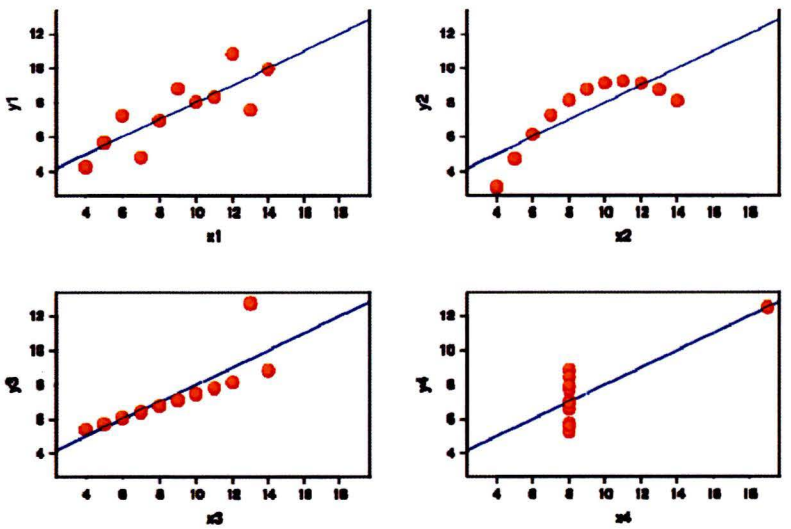

Figure B.2 Different scatter plots with the same ρ (Anscombe, 1973)

This has to be kept in mind when interpreting the statistical values. Therefore, the values R^2 and ρ are used in combination with the corresponding scatter plots to judge the model.

C. Simulation results

C.1 50th WS with rotating and non-rotating T1

Figure C.1 to Figure C.6 show the head responses of the hardware 50th WS (black line) and of the numerical head-neck model of the 50th WS with respect to a non-rotating (blue) as well as rotating T1 coordinate system (magenta). For most responses the difference between the responses with respect to a non-rotating T1 and those with respect to a rotating T1 are negligible.

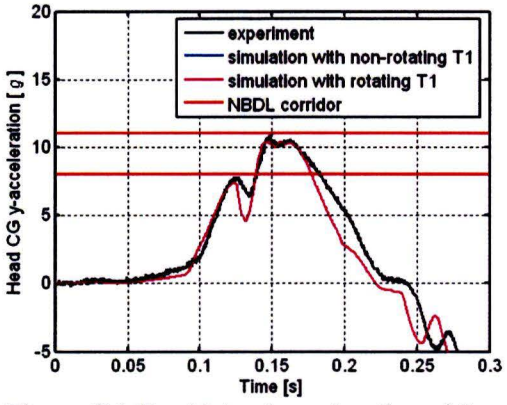

Figure C.1 Head lateral acceleration of the 50th WS in time

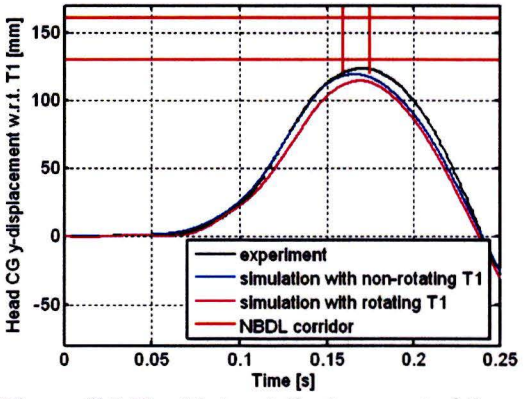

Figure C.2 Head lateral displacement of the 50th WS in time

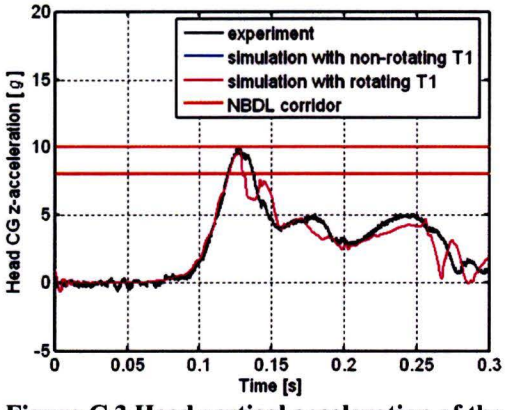

Figure C.3 Head vertical acceleration of the 50th WS in time

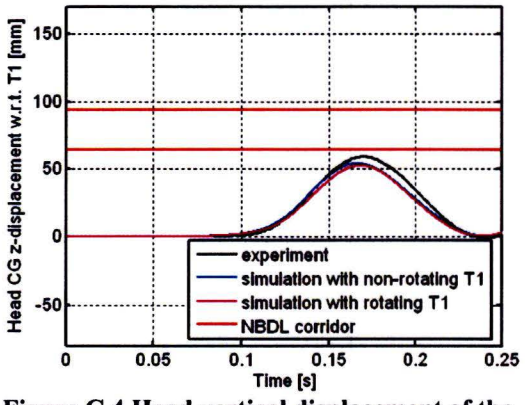

Figure C.4 Head vertical displacement of the 50th WS in time

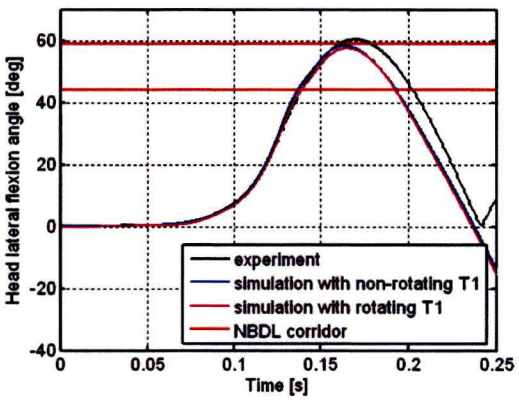

Figure C.5 Head lateral flexion angle of the 50th WS in time

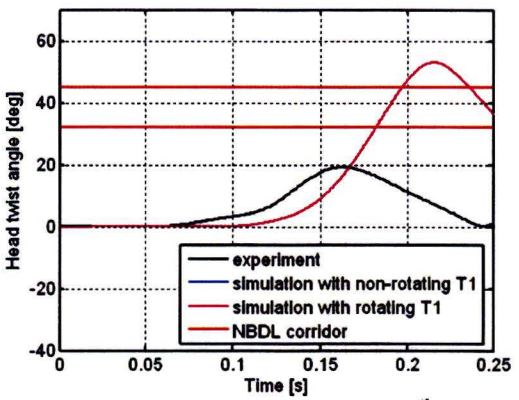

Figure C.6 Head twist angle of the 50th WS in time

C.2 5th WS with rotating and non-rotating T1

Figure C.7 to Figure C.12 show the head responses of the hardware 5th WS (black line) and of the numerical head-neck model of the 5th WS with respect to a non-rotating (blue) as well as rotating T1 coordinate system (magenta). For most responses the difference between the responses with respect to a non-rotating T1 and those with respect to a rotating T1 are negligible.

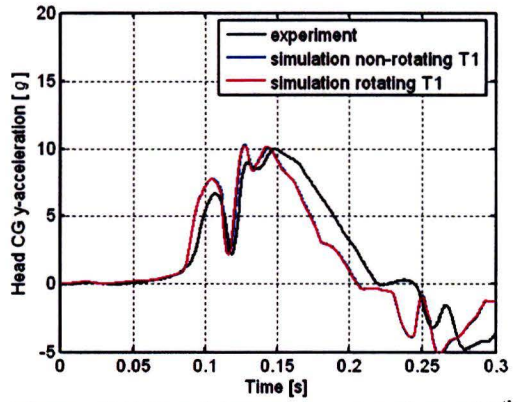

Figure C.7 Head lateral acceleration of 5th WS in time

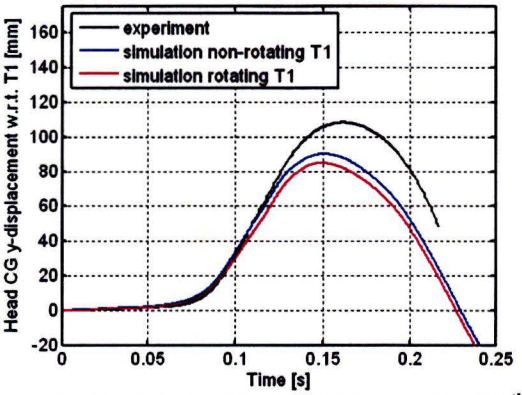

Figure C.8 Head lateral displacement of 5th WS in time

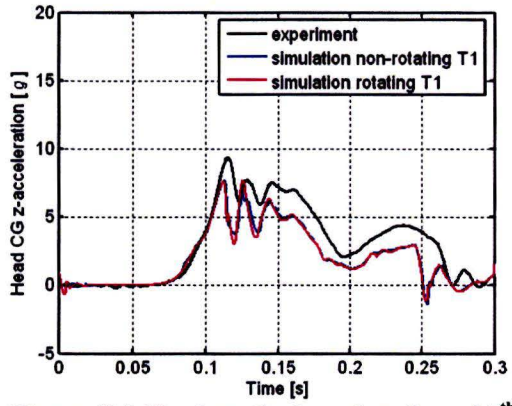

Figure C.9 Head vertical acceleration of 5th WS in time

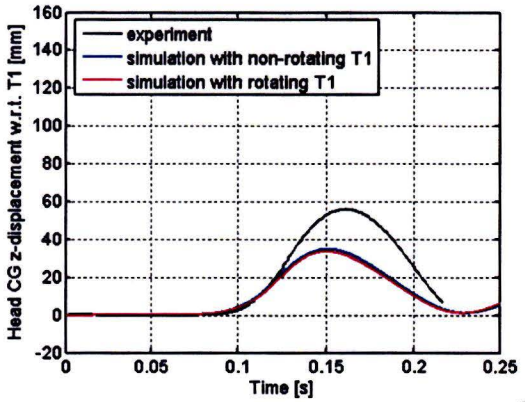

Figure C.10 Head vertical displacement of 5th WS in time

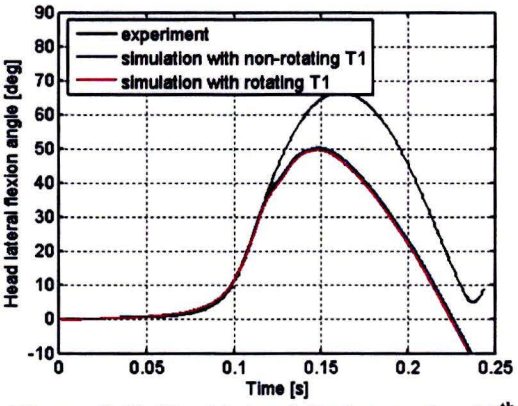

Figure C.11 Head lateral flexion angle of 5th WS in time

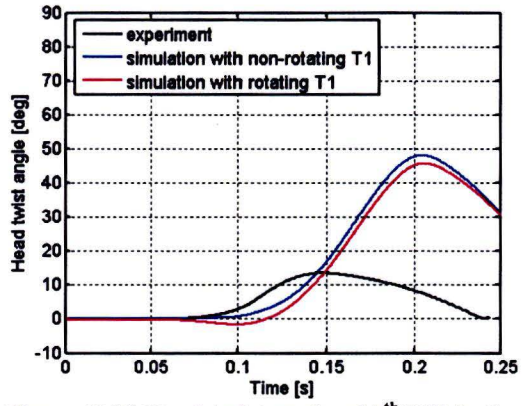

Figure C.12 Head twist angle of 5th WS in time

C.3 5th WS vs. 50th WS: NBDL T1 acceleration

The results of simulations with the numerical head-neck model of the 50th WS (blue) as well as those of simulations with the numerical 5th WS (red) using the T1 pulse, measured during the hardware test of the 50th WS, as input, are displayed in Figure C.13 to Figure C.18. The NBDL response corridors for the 50th WS and the newly developed requirements for the 5th WS are shown as well.

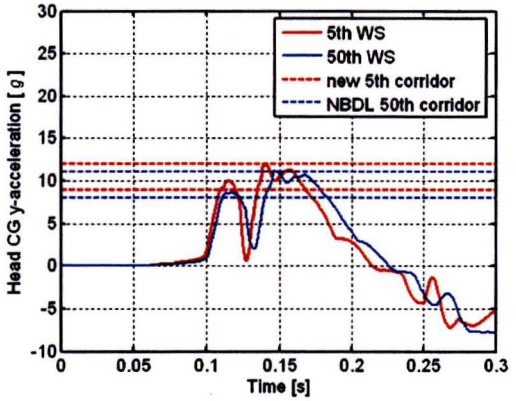

Figure C.13 Head lateral acceleration (input: NBDL T1 acceleration)

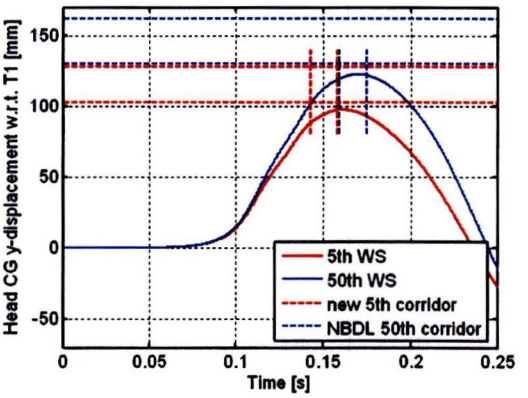

Figure C.14 Head lateral displacement (input: NBDL T1 acceleration)

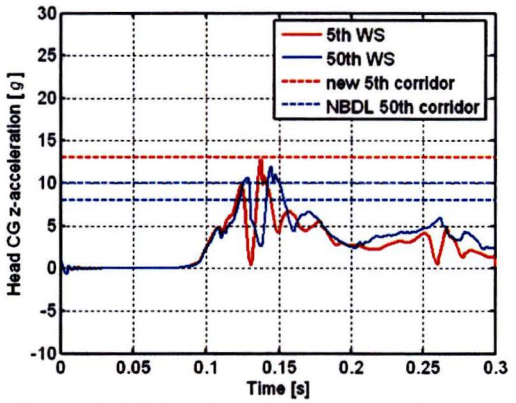

Figure C.15 Head vertical acceleration (input: NBDL T1 acceleration)

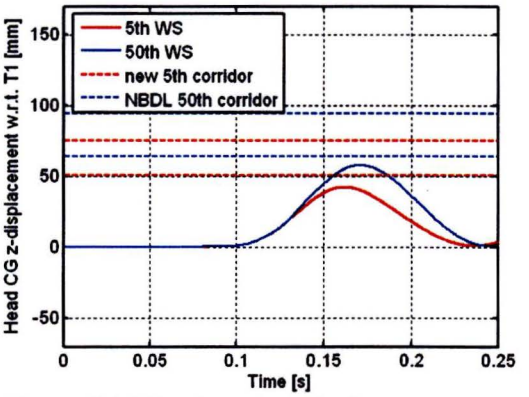

Figure C.16 Head vertical displacement (input: NBDL T1 acceleration)

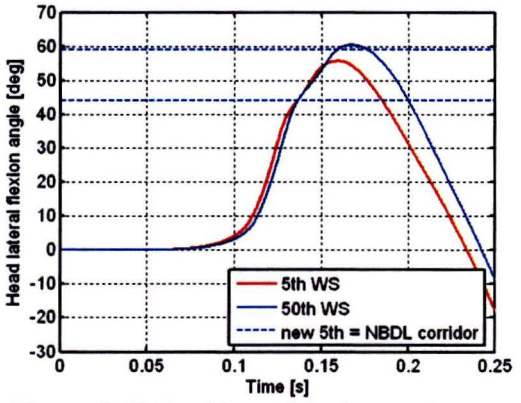

Figure C.17 Head lateral flexion angle (input: NBDL T1 acceleration)

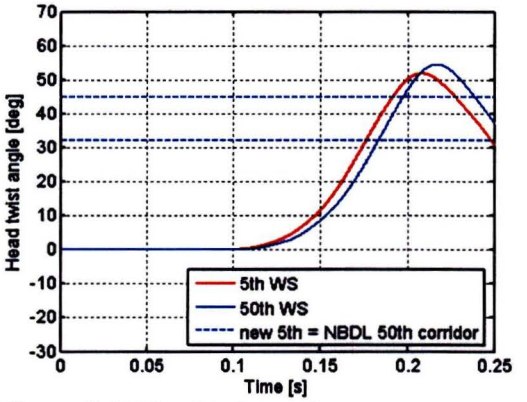

Figure C.18 Head twist angle (input: NBDL T1 acceleration)

C.4 5th WS vs. 50th WS: scaled T1 acceleration

The average T1 accelerations from the experiment with the hardware 50th WS as well as the T1 acceleration for the 5th female scaled according to the method of Irwin, are presented in Figure C.19. They are used as input to the to the numerical head-neck model of the 5th WS, to investigate the influence of a scaled T1 acceleration on the head responses.

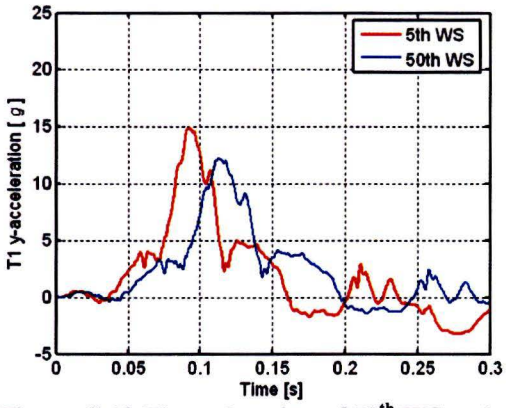

Figure C.19 T1 acceleration of 50th WS and scaled one for 5th WS (Been et al., 2004)

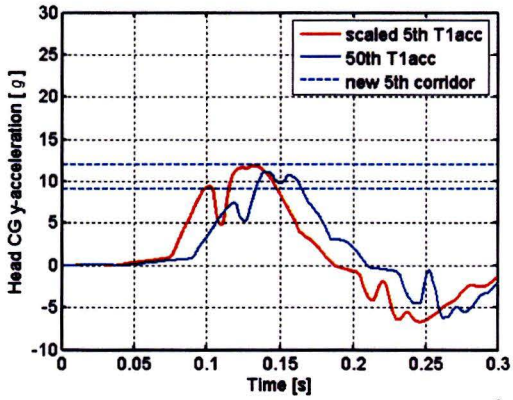

Figure C.20 Head lateral acceleration of 5th WS in time for different T1 acceleration

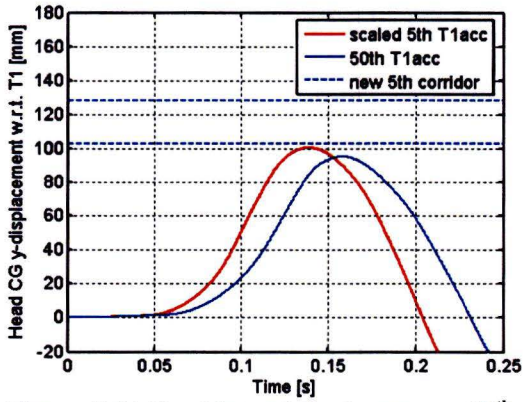

Figure C.21 Head lateral displacement of 5th WS in time for different T1 acceleration

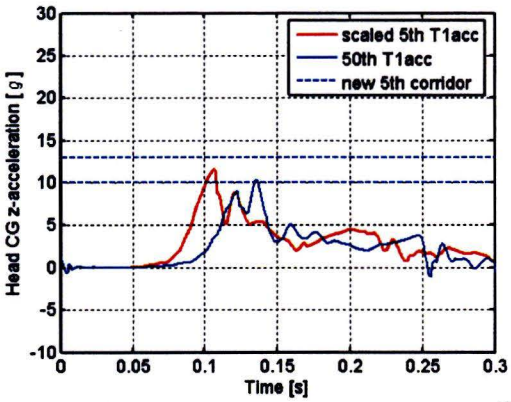

Figure C.22 Head vertical acceleration of 5th WS in time for different T1 acceleration

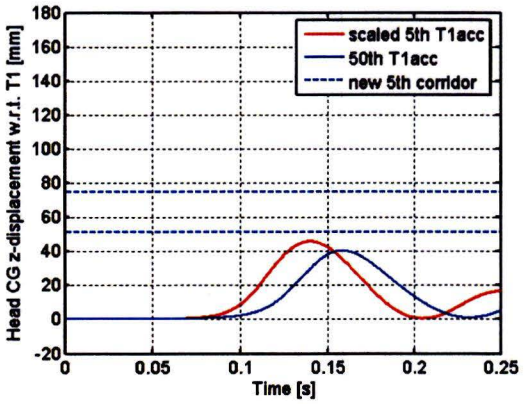

Figure C.23 Head vertical displacement of 5th WS in time for different T1 acceleration

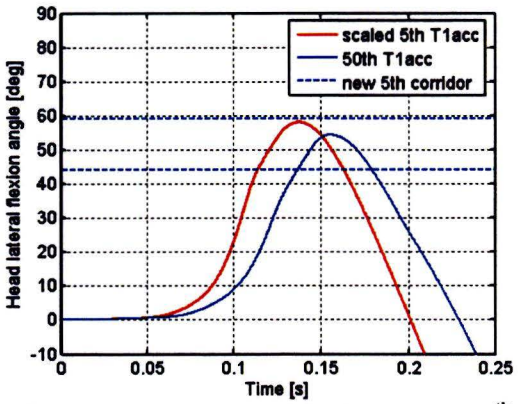

Figure C.24 Head lateral flexion angle of 5th WS in time for different T1 acceleration

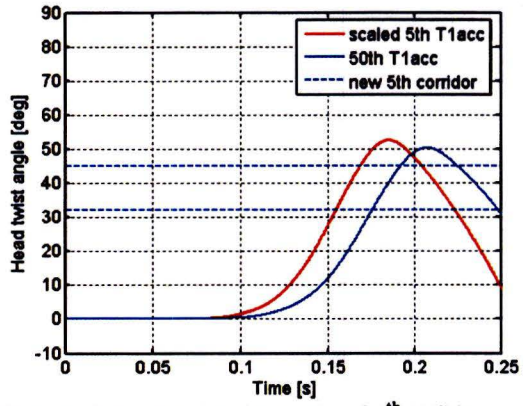

Figure C.25 Head twist angle of 5th WS in time for different T1 acceleration